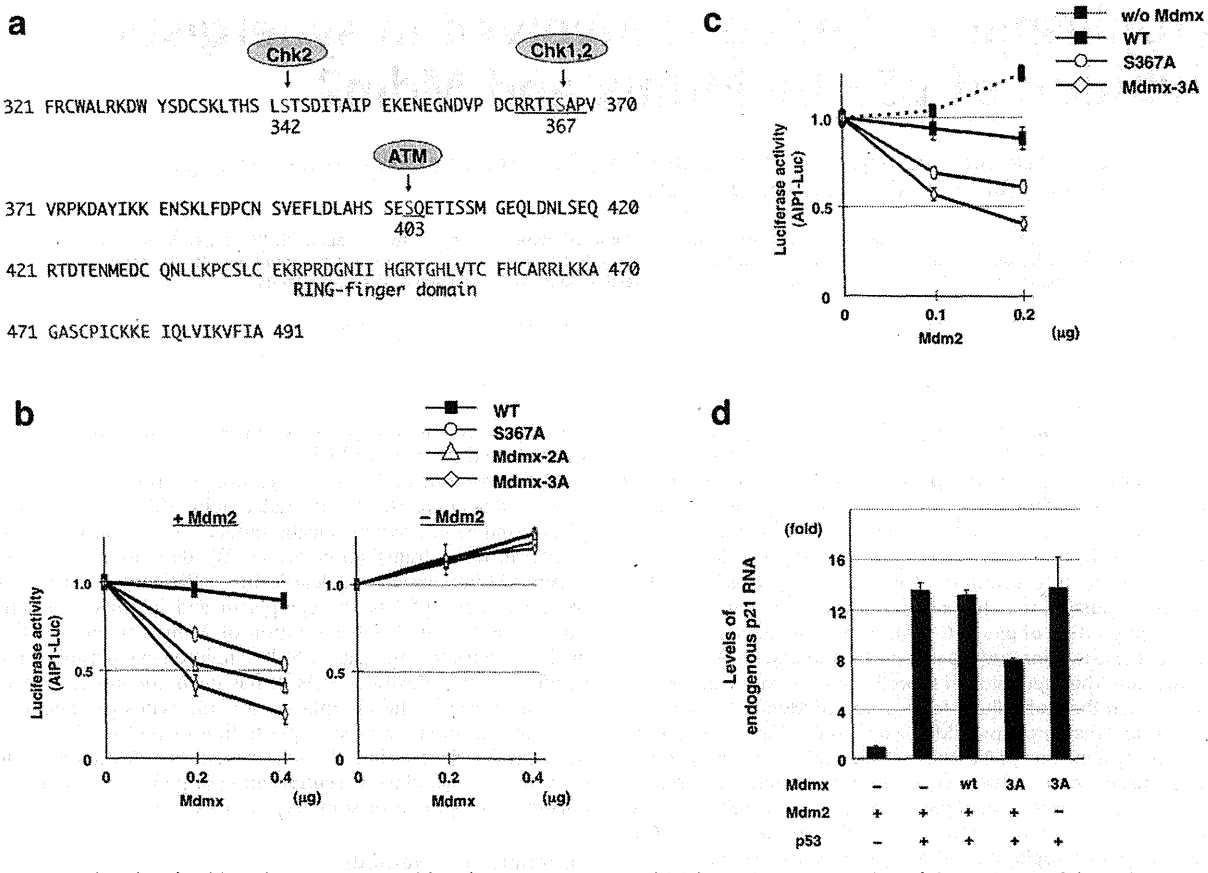

Fig. 1. Non-phosphorylatable Mdmx cooperates with Mdm2 to suppress p53. (a) Schematic representation of the positions of the Mdmx mutations. The serine residues phosphorylated after DNA damage are shown in red. The RING finger domain is shown in blue. (b,c) Inhibition of the transcriptional activity of p53 by the nonphosphorylatable mutants of Mdmx. (b) The indicated amounts of the wild-type Flag-Mdmx or Mdmx mutants were transfected into H1299 cells together with 0.15 μg HA-p53, 0.1 μg AIP-luc, and *Renilla* luciferase in the presence (left panel) or absence (right panel) of 0.2 μg myc-Mdm2. The total amount of transfected DNA was adjusted to 2 μg with pBluescript. Luciferase activity was measured 20 h after transfection. The numbers represent mean values ± standard deviations from experiments carried out in triplicate. The presented values were calculated as follows: value of cells transfected with the indicated amount of Mdmx/value of cells transfected without Mdmx. (c) The indicated amounts of myc-Mdm2 were transfected into H1299 cells together with 0.15 μg HA-p53, AIP-luc, *Renilla* luciferase, in the presence of 0.4 μg control vector, wild-type Flag-Mdmx, or the indicated Mdmx mutant. Luciferase assays were carried out as described in (b). (d) H1299 cells were cotransfected as described in (b). Total RNA prepared from transfected cells was used to measure the levels of endogenous p21 RNA by real-time RT-PCR using Taqman probe (Applied Biosciences, Foster City, CA). Levels of p21 were normalized with those of β-Actin.

shRNA infection. SH-SY5Y cells or IMR-32 cells were infected with lentiviruses as previously described.[21] Cells were infected with the control lentiviruses or the viruses that expressed the specific Mdmx shRNA overnight, incubated for an additional 2 days, and used for western blot analyses or immunostaining.

Additional information on Materials and Methods is provided in the Supporting Information.

Results

Non-phosphorylatable Mdmx effectively cooperates with Mdm2 to suppress p53 activity in H1299. Cellular stresses such as DNA damage cause degradation of Mdmx, via its phosphorylation by damage-induced kinases.[22] Serine 367 (S367) of Mdmx is phosphorylated after DNA damage, and alanine substitution of S367 (S367A), which mimics the nonphosphorylated form, promotes the cooperation between Mdmx and Mdm2 to inhibit p53 activity.[23] In addition to S367, two other serine residues comprise the major phosphorylation sites of Mdmx after DNA damage.[22] One of these sites, serine 403 (S403), is phosphorylated by ATM kinase,[22] whereas its downstream kinases, Chk1 or Chk2, phosphorylate serine 342 (S342) and S367, and facilitate the binding of 14-3-3 to Mdmx[22,24–26] (Fig. 1a). Phosphorylation of each site stimulates the proteasome-mediated degradation of Mdmx via its ubiquitination by Mdm2.[22,23,25]

Assuming that the phosphorylation of S342 and S403, in addition to S367, also compromises p53 suppression by Mdmx, we speculated that additional alanine substitution of S342 and S403 would allow Mdmx to inhibit p53 more effectively. We created the Mdmx mutants with the alanine substitution at S342 (Mdmx-2A) or at S342 plus S403 (Mdmx-3A) in addition to S367A, and introduced each mutant into p53-deficient H1299 cells together with p53 and the p53-responsive luciferase reporter (AIP-luc), in the presence or absence of the transfected Mdm2. Subsequently, the inhibitory effect of each Mdmx mutant on p53 activity was examined (Fig. 1b,c). Low amounts of Mdm2 were transfected so that introduction of Mdm2 alone did not inhibit p53 activity (Fig. 1c). As we reported previously,[23] the S367A mutation augmented the inhibition of p53 activity by Mdmx in the presence of transfected Mdm2 (Fig. 1b,c). The additional alanine substitution at S342 and S403 enhanced the ability of Mdmx to suppress p53 (Fig. 1b,c). In contrast, none of these mutants showed an inhibitory effect on p53 activity in the absence of the transfected Mdm2 (Fig. 1b). We observed similar Mdm2-dependent inhibition

doi: 10.1111/j.1349-7006.2009.01180.x

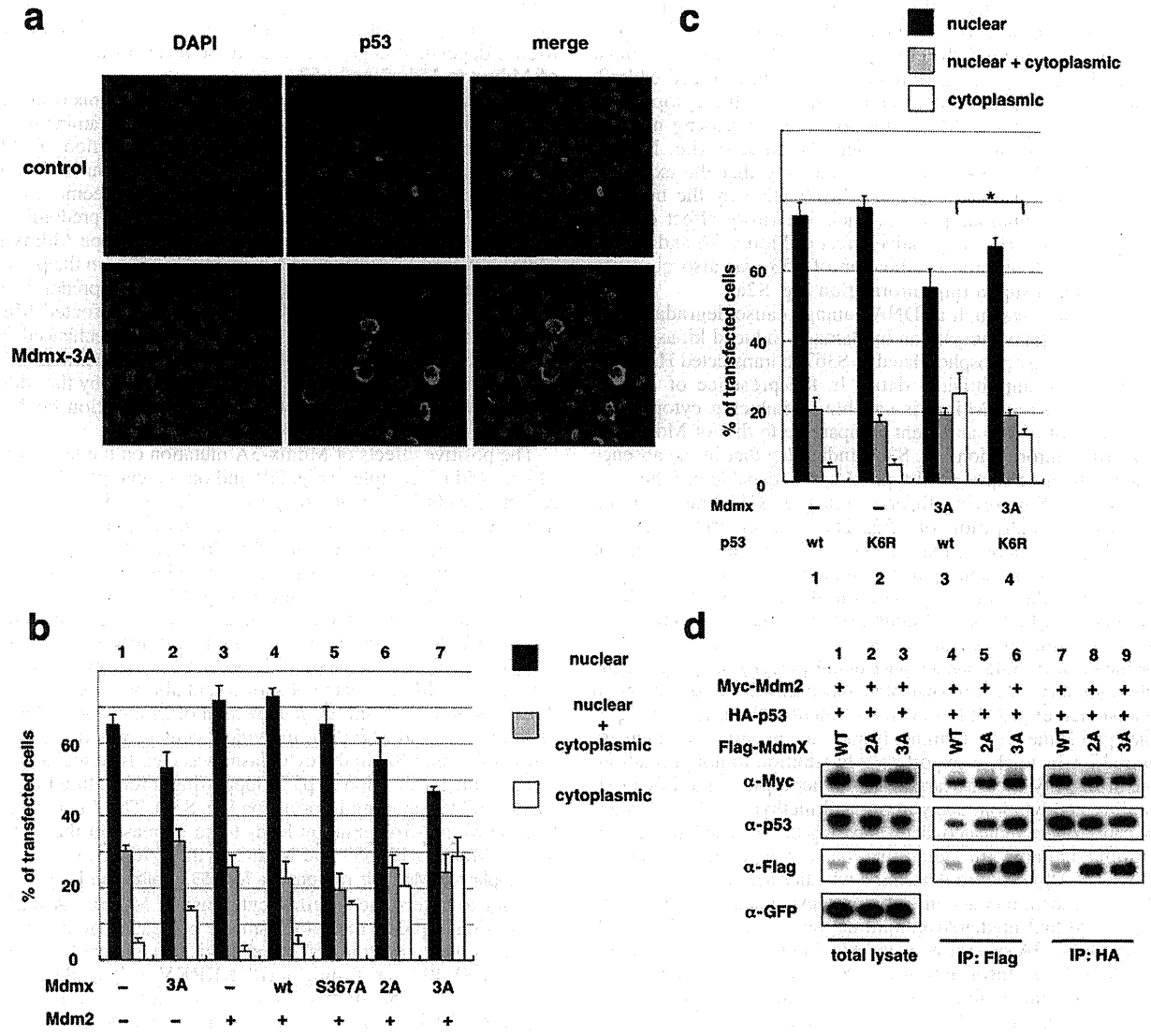

Fig. 2. Non-phosphorylatable Mdmx cooperates with Mdm2 to induce cytoplasmic localization of p53 in H1299. (a) H1299 cells were cotransfected with HA-p53 and myc-Mdm2, in the presence or absence of Mdmx-3A, and used for staining with DAPI and anti-HA antibody. Representative staining of the transfected cells is shown. (b) H1299 cells were cotransfected with the indicated Flag-Mdmx mutants and HA-p53 in the absence (columns 1 and 2) or presence (columns 3–7) of myc-Mdm2, and used for staining with anti-HA antibody. Subcellular localization of p53 of 100 transfected cells was evaluated in triplicate, and the average percentage of cells with the indicated staining pattern of p53 is shown. (c) Wild-type HA-p53 or HA-p53-K6R was transfected into H1299 cells together with myc-Mdm2 in the presence or absence of Flag-Mdmx-3A. Immunostaining analyses were carried out as described in (b). Asterisks indicate statistically significant differences ($P < 0.05$) as given by a one-way ANOVA followed by Tukey post-test. (d) HA-p53, myc-Mdm2, and GFP were transfected into H1299 together with the indicated Flag-tagged Mdmx as described in (b), and lysates prepared from transfected cells were used for immunoprecipitation (IP) with anti-Flag antibody (lanes 4–6) or anti-p53 (DO-1) antibody (lanes 7–9). The total lysates (lanes 1–3) and the immunoprecipitates were analysed by western blot analyses with the indicated antibodies.

of p53 activity by Mdmx-3A on another p53-responsive promoter (Bax-luc) (Supporting Information Fig. S1a). Wild-type Mdmx had an inhibitory effect that was comparable to that of Mdmx-3A in the presence of a chk2 inhibitor (Supporting Information Fig. S1b), suggesting that wild-type Mdmx is capable of inhibiting p53 in the absence of inhibitory phosphorylation.

Cotransfection of Mdm2 with these mutants suppressed the inhibitory effects of p53 on cell growth (Supporting Information Fig. S1c). In accordance with the inhibition of cell growth, Mdmx-3A, but not wild-type Mdmx, inhibits RNA expression of endogenous p21, which is a crucial target of p53 and inhibits cell cycle progression (Fig. 1d). Taken together, these data suggest that non-phosphorylated forms of Mdmx effectively cooperate with Mdm2 to inhibit p53 function.

Non-phosphorylatable Mdmx cooperates with Mdm2 to induce cytoplasmic localization of p53 in H1299. It has been demonstrated that low levels of Mdm2 inhibit p53 by inducing nuclear export.[27] In order to determine whether the nonphosphorylatable mutants of Mdmx cooperate with Mdm2 to inhibit p53 activity by stimulating cytoplasmic localization of p53, we next examined the subcellular localization of p53 after cotransfection of Mdmx, Mdm2, and p53 under the same conditions described in Figure 1(b). Introduction of Mdm2 alone did not significantly affect nuclear localization of p53 (Fig. 2a,b). Although cointroduction of Mdm2 and wild-type Mdmx had only a marginal effect on enhancement of cytoplasmic localization of p53 (Fig. 2b), cointroduction of Mdm2 and Mdmx-3A markedly enhanced a fraction of transfected cells with cytoplasmic p53 staining (Fig. 2a,b). Cytoplasmic

localization of p53 induced by Mdmx-3A alone was much less striking if compared to that induced by Mdm2 and Mdmx-3A (Fig. 2b), indicating that the effect of Mdmx-3A on the subcellular localization is largely dependent on the cointroduced Mdm2. Of note, there was a gradual enhancement of the cytoplasmic localization of p53 as Mdmx harbored an increasing number of alanine mutations at the phosphorylation sites (i.e. Mdmx-wt < S367A < 2A < 3A) (Fig. 2b), indicating that the extent of the stimulation of the cytoplasmic localization by the nonphosphorylatable mutations parallels their inhibitory effect on p53 activity (Fig. 1b). The cooperative effect of Mdmx-3A and Mdm2 to stimulate cytoplasmic localization of p53 was also observed in U2OS cells (Supporting Information Fig. S2a).

Cellular stresses such as DNA damage cause degradation of Mdmx via its phosphorylation by damage-induced kinases.[22,28] Mdmx was highly phosphorylated at S367 in transfected H1299[23] (K. Okamoto, unpublished data). In the presence of a chk2 inhibitor, wild-type Mdmx is capable of inducing cytoplasmic localization of p53 to an extent comparable to that of Mdmx-3A (Supporting Information Fig. S2b), indicating that in the absence of the inhibitory kinase, wild-type Mdmx is capable of inhibiting p53 activity (Supporting Information Fig. S1b) and inducing cytoplasmic localization of p53. These observations suggest that Mdmx phosphorylation may occur during the procedure of DNA transfection, and that the nonphosphorylatable Mdmx mutation facilitates clear observation of the cooperative effects of Mdmx and Mdm2 on p53 inhibition, by negating the inhibitory effects of Mdmx phosphorylation.

Mutation at the C-terminal lysines of p53 partially compromises the inhibitory effects of Mdmx-mediated enhancement of ubiquitination and inhibition of p53. It has been documented that Mdm2 ubiquitinates p53 at the six C-terminal lysines, the integrity of which are required for its nuclear export.[29,30] In addition to ubiquitination, some of these lysines are targeted for other types of modification, including neddylation, acetylation, and methylation.[31,32] Recent publications have indicated that Mdmx rescues the catalytic activity of Mdm2 mutants for ubiquitination and neddylation of p53 *in vivo*.[18,19,33] In order to determine whether Mdmx-3A enhances Mdm2-dependent p53 ubiquitination, we examined whether Mdmx enhances Mdm2-mediated ubiquitination in transfected H1299. Indeed, Mdmx-3A synergized with Mdm2 to induce p53 ubiquitination (Supporting Information Fig. S2c). In order to determine whether cooperative ubiquitination targets the C-terminal lysines of p53 by Mdmx and Mdm2, we created a mutant p53 in which all six lysines at the C-terminal domain were substituted with arginine (p53-K6R). *In vivo* ubiquitination assays confirmed that the K6R mutation eliminates the majority of p53 ubiquitination in transfected H1299 (data not shown). The K6R mutation partially inhibited Mdmx-3A-mediated cytoplasmic localization of p53 (Fig. 2c) and transcriptional inhibition of p53 (Supporting Information Fig. S2d). Thus, modification of the six lysines is partly required for Mdmx-dependent cytoplasmic localization and inactivation of p53, yet there exist other mechanisms by which Mdmx and Mdm2 cooperate to suppress p53 function.

Non-phosphorylatable mutations of Mdmx increase levels of the association of Mdmx to Mdm2 and p53. Next we determined whether the nonphosphorylatable mutations of Mdmx affect the levels of transfected p53, Mdm2, and Mdmx as well as the interaction among them (Fig. 2d). Mdmx-2A or Mdmx-3A expression did not markedly decrease the levels of p53 (Fig. 2d). In contrast, both the Mdmx-2A and Mdmx-3A mutations clearly increased the levels of introduced Mdmx (Fig. 2d). The levels of wild-type Mdmx and the Mdmx mutants were comparable in the presence of a proteasomal inhibitor MG132 (Supporting Information Fig. S2e), suggesting that the nonphosphorylatable mutations render Mdmx less sensitive to Mdm2-dependent proteasomal degradation.[22] In accordance with increased levels of Mdmx-2A and Mdmx-3A, the Mdmx mutations led to increased levels of the association of Mdmx to Mdm2 and p53 (Fig. 2d). These results indicate that the nonphosphorylatable mutations, by protecting Mdmx from Mdm2-dependent degradation, increase levels of the association of Mdmx to Mdm2 and p53.

Mdmx-3A mutation stimulates the association of Mdmx with Mdm2 and p53 predominantly in the cytoplasm. In order to examine whether the Mdmx-3A mutation affects subcellular localization of Mdmx and/or Mdm2 as well as p53, we next carried out immunostaining analyses of transfected Mdm2 and Mdmx. In agreement with a previous report,[10] transfected wild-type Mdmx was predominantly localized to the cytoplasm (Fig. 3a). Both wild-type Mdmx and Mdmx-3A mainly remained in the cytoplasm either in the presence or absence of cotransfected Mdm2 (Fig. 3a). Mdm2 predominantly localized to the nucleus in the absence of transfected Mdmx (Fig. 3b). Cotranfection of wild-type Mdmx mildly enhanced cytoplasmic localization of introduced Mdm2, and the extent of the cytoplasmic localization was markedly augmented by the Mdmx-3A mutation (Fig. 3b). Thus, the Mdmx-3A mutation facilitates cytoplasmic localization of cointroduced Mdm2.

The positive effects of Mdmx-3A mutation on the levels of the Mdmx–Mdm2 complex (Fig. 2d) and on the cytoplasmic localization of Mdm2 (Fig. 3b) suggest that the mutation leads to an increase of the Mdmx–Mdm2 complex in cytoplasm. Therefore, we next examined the extent of their interaction in each subcellular compartment after subcellular fractionation. In agreement with the results of the immunostaining (Fig. 3a,b), both Mdmx-3A and Mdm2 were mainly localized to the cytoplasm, and the Mdmx-3A–Mdm2 complex was predominantly formed in the cytoplasm (Fig. 3c). Cytoplasmic Mdmx-3A clearly colocalized with not only Mdm2 (data not shown) but also with p53 (Fig. 3d). Analyses of the subcellular localization of Mdmx-3A and p53 or of Mdmx-3A and Mdm2 in individual cells revealed that localization of Mdmx-3A in the cytoplasm was clearly associated with cytoplasmic localization of p53 (Supporting Information Fig. S3a) and Mdm2 (Supporting Information Fig. S3b). These data indicate that the Mdmx-3A mutation leads to an increase in the association of Mdmx with p53 and Mdm2 in the cytoplasm.

Cytoplasmic Mdmx is responsible for p53 localization in cytoplasm. In order to determine whether cytoplasmic Mdmx-3A induces localization of p53 to the cytoplasm, we generated Mdmx mutants in which either a peptide that corresponds to a nuclear localization signal of SV40 large T antigen (PKKKRKV) or a nuclear export signal of Rev of human immunodeficiency virus type-1 (LQLPPLERLTL) was connected to Mdmx-3A (NLS-Mdmx-3A or NES-Mdmx-3A). Subsequently, we introduced these Mdmx mutants together with Mdm2 and p53, and evaluated the effect of subcellular localization of Mdmx-3A on Mdm2 and p53. As expected, NLS-Mdmx-3A and NES-Mdmx-3A showed predominant localization to nuclei and cytoplasm respectively (Fig. 4a,b). Clear cytoplasmic localization of Mdm2 (Fig. 4c) and p53 (Fig. 4d) was induced by NES-Mdmx-3A, but not by NLS-Mdmx-3A. Inhibition of transcriptional activity of p53 by Mdmx-3A was enhanced by NES-Mdmx-3A and rather reduced by NLS-Mdmx-3A (Fig. 4e). Thus, cytoplasmic Mdmx-3A tethers p53 to the cytoplasm, whereas it effectively inhibits p53 activity in transfected H1299 cells.

Mdmx in the cytoplasm promotes cytoplasmic retention of endogenous p53. Next we examined whether subcellular localization of Mdmx-3A dictates localization of endogenous p53. Wild-type Mdmx, Mdmx-3A, NES-Mdmx-3A, or NLS-Mdmx-3A was introduced into U2OS cells, in which wild-type p53 is expressed predominantly in nuclei,[34] and we determined whether the mutants affect the subcellular localization of endogenous p53. The Mdmx-3A mutants were expressed at comparable levels (Fig. 4f). As we observed in H1299, NLS-Mdmx-3A and NES-Mdmx-3A predominantly localized to nuclei and cytoplasm respectively (data not shown). Introduction of wild-type Mdmx did not significantly affect nuclear localization of p53. In contrast, introduction of the

doi: 10.1111/j.1349-7006.2009.01180.x

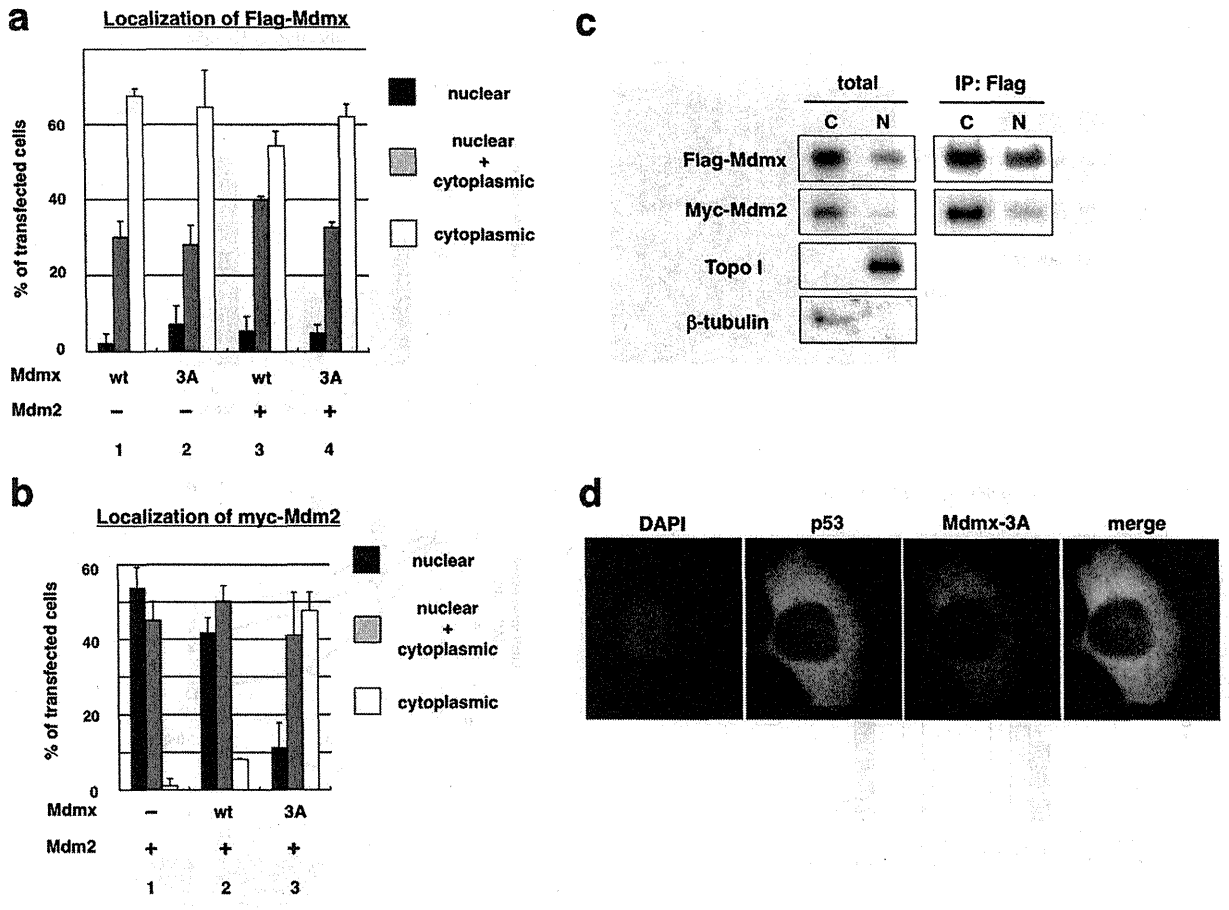

Fig. 3. The Mdmx-3A mutation stimulates the localization of Mdm2 and p53 predominantly to the cytoplasm. (a,b) HA-p53 was transfected into H1299 cells together with the indicated Flag-Mdmx in the presence or absence of myc-Mdm2 as described in Figure 2(b). The transfected cells were sequentially immunostained with (a) anti-Flag (M2) antibody or (b) antimyc antibody, antimouse IgG antibody conjugated with Alexa 595, and anti-HA antibody conjugated with Alexa 488 (Molecular Probe). Subcellular localization of (a) Flag-Mdmx or (b) myc-Mdm2 in cells that express HA-p53 was evaluated as described in Figure 2(b). (c) H1299 cells were transfected with HA-p53 together with Flag-Mdmx-3A and myc-Mdm2. The transfected cells were subjected to subcellular fractionation. The total lysates and the Flag-immunoprecipitates were then used for western blot analyses with the indicated antibodies. Topoisomerase I and γ tubulin are shown as nuclear and cytoplasmic markers respectively. (d) Representative staining of cells that express cytoplasmic p53 and Mdmx.

Mdmx-3A mutants induced localization of p53 to the cytoplasm, and a striking enhancement of cytoplasmic localization of p53 was observed in the presence of NES-Mdmx-3A (Fig. 4f). Taken together, these data indicate that cytoplasmically located Mdmx, presumably by tethering p53, induces localization of endogenous p53 to the cytoplasm.

Both Mdmx and Mdm2 predominantly localize to the cytoplasm of neuroblastoma cells. Inactivation of p53 via its cytoplasmic localization is frequently observed in some types of cancer such as neuroblastoma,[35] and yet the precise mechanism by which p53 is sequestered in cytoplasm remains obscure. It was reported that Mdm2 mediates the cytoplasmic retention of p53 in neuroblastoma.[36,37] In order to examine whether Mdmx as well as Mdm2 is involved in p53 inactivation via cytoplasmic sequestration in neuroblastoma, we analyzed SH-SY5Y and IMR-32 cells that, like most other neuroblastoma cells, harbor wild-type p53 with cytoplasmic localization (Fig. 5a; Supporting Information Fig. S4a). Expression levels of Mdmx in SH-SY5Y were much higher than those in normal human fibroblasts, and even higher than those in MCF-7 (data not shown), breast cancer cells in which the *mdmx* gene is amplified and Mdmx is expressed at high levels.[38] Both Mdmx and Mdm2 predominantly localized to the cytoplasm in SH-SY5Y cells (Supporting Information Fig. S4a). The extent of S367 phosphorylation in SH-5YSY cells was much lower than that in the transfected H1299 cells (Supporting Information Fig. S4c). These observations suggest that Mdmx is expressed, probably in nonphosphorylated forms, at high levels in the cytoplasm in unstressed SH-SY5Y cells.

Nuclear Mdmx inhibits cytoplasmic retention of p53 in SH-SY5Y. In order to determine whether subcellular localization of Mdmx-3A dictates localization of endogenous p53 in neuroblastoma cells as well as in U2OS cells, the effects of subcellular localization of wild-type Mdmx or the Mdmx mutants on endogenous p53 localization were evaluated as described in Figure 4(f). The Mdmx-3A mutants were expressed at comparable levels (Fig. 5b). In accordance with cytoplasmic localization of endogenous Mdmx (Supporting Information Fig. S4a), Mdmx-3A and wild-type Mdmx exclusively localized to the cytoplasm (Fig. 5b). As expected, the majority of NLS-Mdmx-3A localized to nuclei (87%) and NES-Mdmx-3A totally localized to the cytoplasm. Immunostaining of transfected SH-SY5Y cells revealed that the expression of NLS-Mdmx-3A, but not NES-Mdmx-3A, reduced cytoplasmic localization of p53 (Fig. 5b), indicating that nuclear expression of Mdmx-3A inhibits cytoplasmic retention of p53 in SH-SY5Y.

Mdmx is required for inactivation of p53 in neuroblastoma cells. In order to further examine the role of Mdmx in p53 inactivation

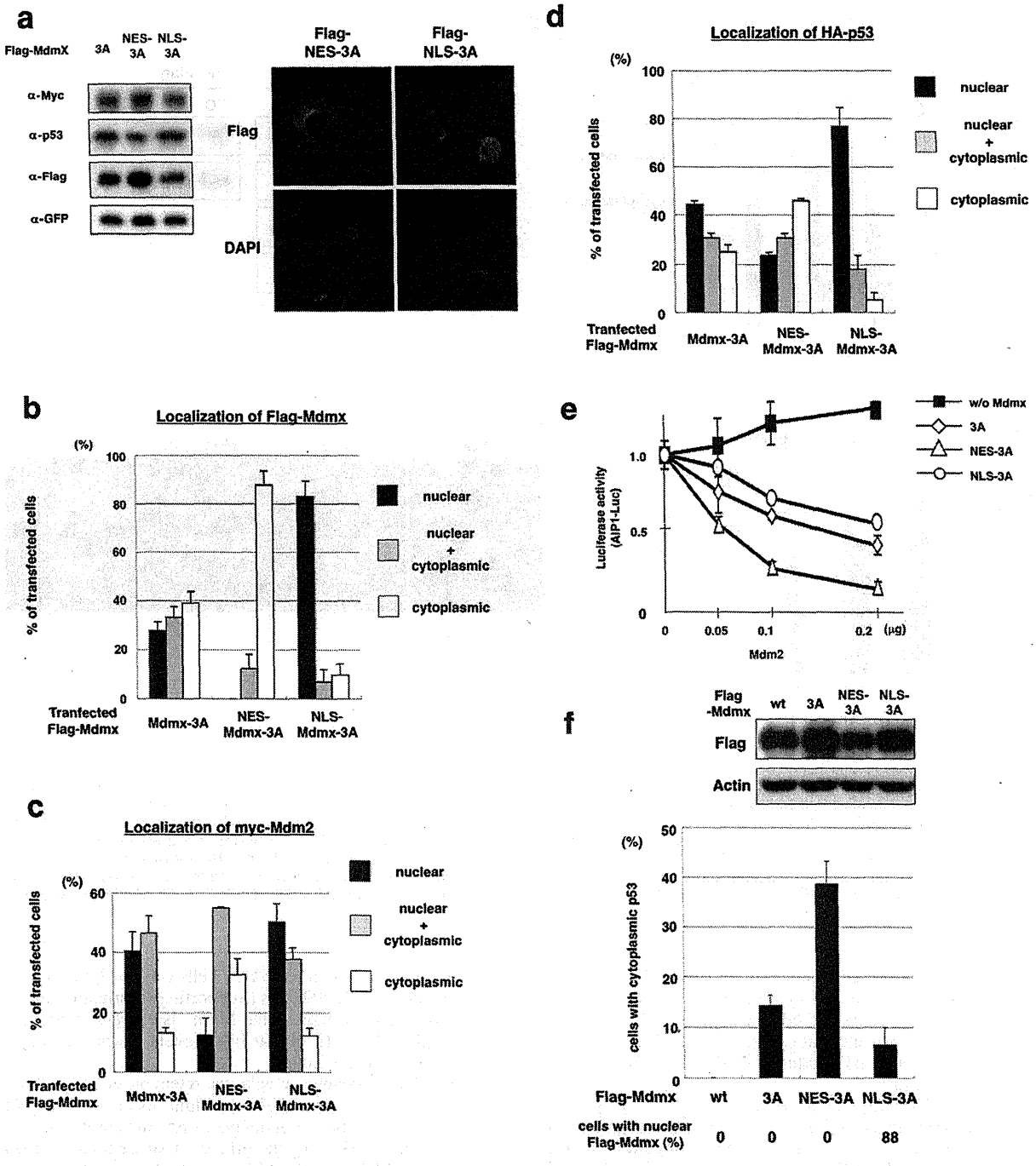

Fig. 4. Cytoplasmic Mdmx tethers p53 and Mdm2 to the cytoplasm and stimulates p53 inhibition. (a) H1299 cells were cotransfected with HA-p53, myc-Mdm2, GFP, and the indicated Flag-tagged Mdmx. Left panel, western blot analyses with the indicated antibodies. Right panel, representative staining with anti-Flag antibody and DAPI. (b–d) H1299 cells were transfected with the indicated Mdmx, together with myc-Mdm2, and immunostained with (b) anti-Flag antibody, (c) anti-Mdm2 antibody, or (d) anti-HA antibody. Subcellular localization of transfected (b) Mdmx, (c) Mdm2, or (d) p53 was represented as described in Figure 2(b). (e) Flag-Mdmx mutant or the control vector was transfected into H1299 cells together with HA-p53, in the presence of the indicated amounts of myc-Mdm2, and luciferase assays were carried out as described in Figure 1(c). (f) U2OS cells were transfected with the indicated Flag-Mdmx. Upper panel, western blot analyses with the anti-Flag or the anti-actin antibodies. Lower panel, cells transfected with the indicated plasmids were immunostained with the anti-Flag and antip53 (CM1) antibodies, and a fraction of the transfected cells with cytoplasmic p53 staining was quantified.

in neuroblastoma cells, we inhibited Mdmx expression by infecting cells with the lentiviruses expressing Mdmx shRNA. Mdmx inhibition by the specific shRNA, while not significantly affecting levels of p53, induced expression of p21, a crucial p53 target (Fig. 5c) and reduced the cytoplasmic localization of p53 (Fig. 5d,e). The positive role of Mdmx in cytoplasmic localization of p53 was confirmed by western blot analyses of nuclear and cytoplasmic lysates prepared from the infected cells. Depletion of Mdmx

doi: 10.1111/j.1349-7006.2009.01180.x

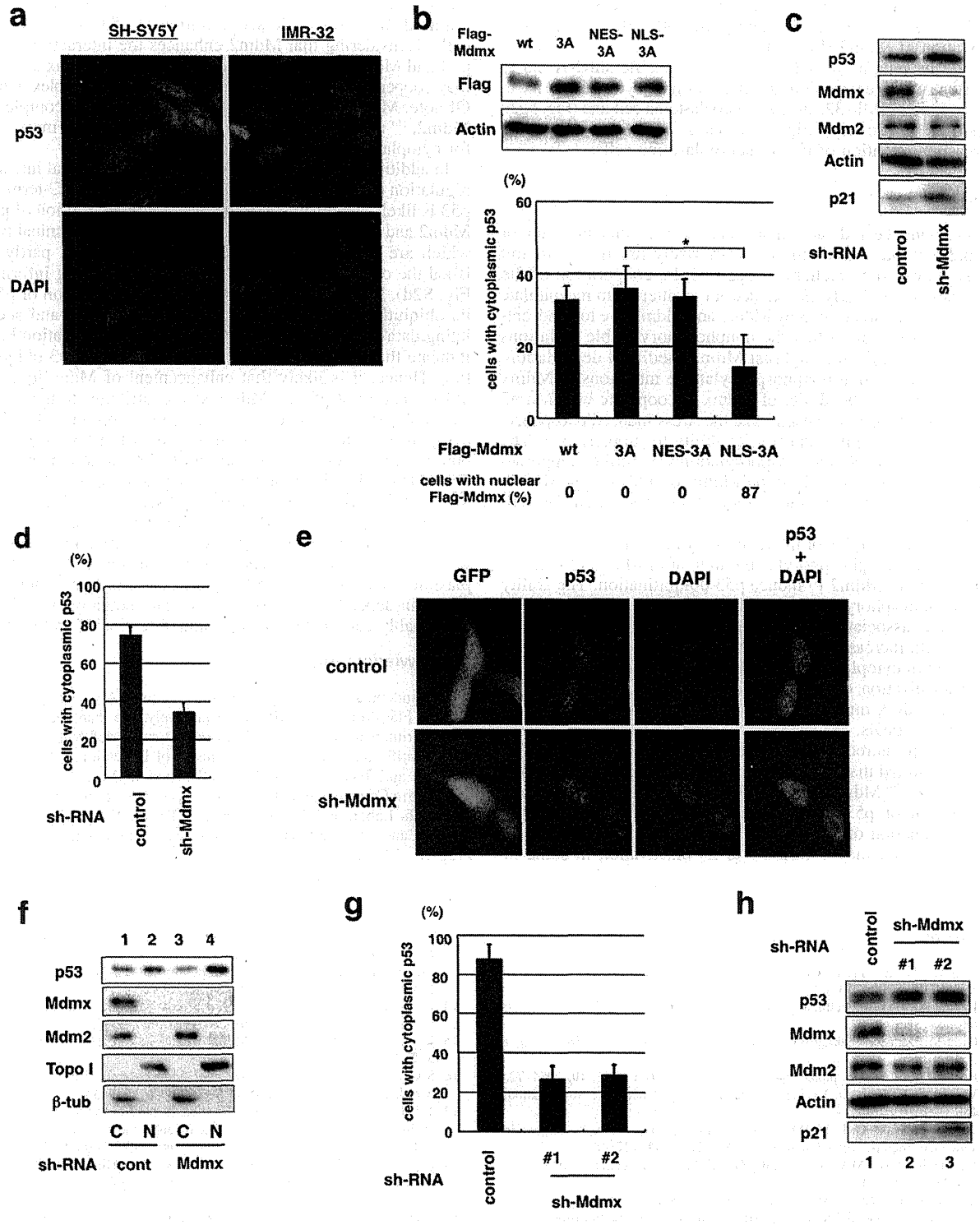

Fig. 5. Mdmx is required for cytoplasmic retention of p53 in neuroblastoma cells. (a) Cytoplasmic retention of p53 in neuroblastoma. SH-SY5Y or IMR-32 cells were stained with antip53 antibody (CM1) and DAPI. (b) SH-SY5Y cells were transfected with the indicated Flag-tagged Mdmx. Western blot analyses and quantification of a fraction of cells with cytoplasmic p53 were carried out as described in Figure 4(f). (c–f) SH-SY5Y cells were infected with the control lentivirus or the viruses expressing Mdmx shRNA. (c) Lysates prepared from the infected cells were used for western blot analyses with the indicated antibodies. (d) The infected cells were immunostained with antip53 polyclonal antibody (CM1) and DAPI. The average percentage of the infected cells with cytoplasmic staining of p53 was presented after evaluating subcellular localization of p53 of 100 cells in triplicate. (e) Representative pictures of staining of cells that were infected with the control lentiviruses or the viruses that express Mdmx shRNA. Note that the viruses express GFP, and infection efficiency is ~100% judging from GFP expression. (f) Subcellular fractionation and western blot analyses were carried out with the indicated antibodies. (g,h) IMR-32 cells were infected with the control lentiviruses or the viruses that express Mdmx shRNA, and (g) western blot analyses or (h) the quantification of subcellular distribution of p53 was carried out as described in (c) and (d) respectively.

decreased p53 levels in the cytoplasm and increased those in nuclei, while the depletion did not significantly affect cytoplasmic localization of Mdm2 (Fig. 5f).

Similarly, inhibition of Mdmx by the specific shRNA led to induction of p21 expression and inhibition of cytoplasmic localization of p53 in IMR-32, another neuroblastoma cell line (Fig. 5g,h; Supporting Information Fig. S4c). Thus, Mdmx contributes to cytoplasmic retention of p53 in neuroblastoma cells.

Discussion

Genetic evidence indicates that *mdmx* is a crucial inhibitor of p53 and that *mdmx* and *mdm2* cooperatively function to inhibit p53. However, the mechanical basis of the cooperation of the oncogenes is not clearly established. In an attempt to recapitulate synergistic inhibition of p53 by Mdmx and Mdm2, we took advantage of our observation that the nonphosphorylatable mutations confer Mdmx resistance against Mdm2-mediated degradation. We demonstrated that nonphosphorylatable mutations of Mdmx markedly enhance the ability of Mdmx to cooperate with Mdm2 for inhibition of p53, suggesting that the stress-induced phosphorylation of Mdmx is important for its ability to suppress p53. The importance of the Mdmx phosphorylation was further supported by the functionality of wild-type Mdmx on p53 suppression in the presence of a chk2 inhibitor (Supporting Information Figs S1b and 2b).

Through the analyses of the function of the Mdmx mutants, we found that the nonphosphorylatable mutant of Mdmx effectively cooperates with Mdm2 to induce p53 ubiquitination. The ability of the nonphosphorylatable mutations of Mdmx to inhibit p53 activity was associated with enhanced cytoplasmic retention of p53 and with increased levels of the interaction of Mdmx to p53 and Mdm2 in cytoplasm. A causal role of cytoplasmic Mdmx to induce localization of p53 in the cytoplasm was demonstrated using the Mdmx mutants that harbor autonomous subcellular localization signals.

p53 is sequestered in the cytoplasm in some types of cancer, and it is assumed that the sequestration of p53 contributes to p53 inactivation.[35,39] Mdm2 is essential for inhibition and cytoplasmic sequestration of p53 in neuroblastoma cells,[36,37] and the cooperative function of Mdmx and Mdm2 to induce p53 retention in the cytoplasm may contribute to its inactivation in some of cancer cells. We found that, in addition to Mdm2, Mdmx is also required for cytoplasmic sequestration of p53 in neuroblastoma cells. Considering that Mdm2 enhances the interaction between p53 and Mdmx in the transfected H1299 cells, Mdmx and Mdm2 may cooperate by stimulating the formation of a complex with p53. Of note, Mdmx stabilizes p53 via a formation of a complex with Mdm2,[16] and formation of such a stable complex may account for cytoplasmic sequestration of p53.

In addition to the cytoplasmic tethering via physical interaction, regulation of post-translational modification of the C-terminal of p53 is likely to contribute to the cooperative inhibition of p53 by Mdm2 and Mdmx, because mutations in the six C-terminal lysines, which are targets for the regulatory modification, partly abolished the cooperative inhibition of p53 (Supporting Information Fig. S2d). Mdm2 promotes cytoplasmic translocation of p53 via its ubiquitination at the same lysine residues,[27,40] and accumulating data[9,18,19] as well as ours (Supporting Information Fig. 2c) indicate that Mdmx promotes Mdm2-dependent p53 ubiquitination. Hence, it is likely that enhancement of Mdm2-dependent ubiquitination of p53 by Mdmx also contributes to the cooperative inhibition of p53 activity by these oncoproteins. In fact, the cytoplasmic retention of p53 in neuroblastoma is in part attributed to multimono-ubiquitination of p53 due to defective function of HAUSP, a de-ubiquitinating enzyme for p53 and Mdmx and Mdm2.[34,41,42] However, we did not observe a significant change in the pattern of p53 laddering, which presumably represents ubiquitinated p53, in neuroblastoma cells after knock down of Mdmx (data not shown). The two mechanisms that mediate cytoplasmic localization of p53, namely cytoplasmic tethering and ubiquitin-dependent translocation, are not mutually exclusive, and presumably contribute to cytoplasmic retention of p53 by Mdmx.

Acknowledgments

We are indebted to Jiandong Chen and Hirofumi Arakawa for providing us with Flag-Mdm2 and AIP-luc respectively. We thank Kenji Kashima for experimental assistance. This work was supported by a Grant-in-Aid for Scientific Research from the Ministry of Education, Culture, Sports, Science, and Technology of Japan (Y.T. and K.O.), a Grant-in-Aid for Third Term Comprehensive Control Research for Cancer from the Ministry of Health, Labor, and Welfare, Japan (Y.T.), the Foundation for Promotion of Cancer Research (K.O.), and the Japan–France Integrated Action Program (K.O. and C.G.).

References

1 Braithwaite AW, Prives CL. p53: more research and more questions. *Cell Death Differ* 2006; **13**: 877–80.
2 Levine AJ. p53, the cellular gatekeeper for growth and division. *Cell* 1997; **88**: 323–31.
3 Oren M. Decision making by p53: life, death and cancer. *Cell Death Differ* 2003; **10**: 431–42.
4 Ko LJ, Prives C. p53: puzzle and paradigm. *Genes Dev* 1996; **10**: 1054–72.
5 Vogelstein B, Lane D, Levine AJ. Surfing the p53 network. *Nature* 2000; **408**: 307–10.
6 Toledo F, Wahl GM. MDM2 and MDM4: p53 regulators as targets in anticancer therapy. *Int J Biochem Cell Biol* 2007; **39**: 1476–8.
7 Marine JC, Dyer MA, Jochemsen AG. MDMX: from bench to bedside. *J Cell Sci* 2007; **120**: 371–8.
8 Marine JC, Francoz S, Maetens M, Wahl G, Toledo F, Lozano G. Keeping p53 in check: essential and synergistic functions of Mdm2 and Mdm4. *Cell Death Differ* 2006; **13**: 927–34.
9 Linares LK, Hengstermann A, Ciechanover A, Muller S, Scheffner M. HdmX stimulates Hdm2-mediated ubiquitination and degradation of p53. *Proc Natl Acad Sci USA* 2003; **100**: 12 009–14.
10 Gu J, Kawai H, Nie L *et al.* Mutual dependence of MDM2 and MDMX in their functional inactivation of p53. *J Biol Chem* 2002; **277**: 19 251–4.
11 Tanimura S, Ohtsuka S, Mitsui K, Shirouzu K, Yoshimura A, Ohtsubo M. MDM2 interacts with MDMX through their RING finger domains. *FEBS Lett* 1999; **447**: 5–9.
12 Sharp DA, Kratowicz SA, Sank MJ, George DL. Stabilization of the MDM2 oncoprotein by interaction with the structurally related MDMX protein. *J Biol Chem* 1999; **274**: 38 189–96.
13 Michael D, Oren M. The p53–Mdm2 module and the ubiquitin system. *Semin Cancer Biol* 2003; **13**: 49–58.
14 Honda R, Tanaka H, Yasuda H. Oncoprotein MDM2 is a ubiquitin ligase E3 for tumor suppressor p53. *FEBS Lett* 1997; **420**: 25–7.
15 Coutts AS, La Thangue NB. Mdm2 widens its repertoire. *Cell Cycle* 2007; **6**: 827–9.
16 Stad R, Little NA, Xirodimas DP *et al.* Mdmx stabilizes p53 and Mdm2 via two distinct mechanisms. *EMBO Rep* 2001; **2**: 1029–34.
17 Toledo F, Krummel KA, Lee CJ *et al.* A mouse p53 mutant lacking the proline-rich domain rescues Mdm4 deficiency and provides insight into the Mdm2-Mdm4-p53 regulatory network. *Cancer Cell* 2006; **9**: 273–85.
18 Poyurovsky MV, Priest C, Kentsis A *et al.* The Mdm2 RING domain C-terminus is required for supramolecular assembly and ubiquitin ligase activity. *EMBO J* 2007; **26**: 90–101.
19 Uldrijan S, Pannekoek WJ, Vousden KH. An essential function of the extreme C-terminus of MDM2 can be provided by MDMX. *EMBO J* 2007; **26**: 102–12.
20 Shinozaki T, Nota A, Taya Y, Okamoto K. Functional role of Mdm2 phosphorylation by ATR in attenuation of p53 nuclear export. *Oncogene* 2003; **22**: 8870–80.
21 Laurie NA, Donovan SL, Shih CS *et al.* Inactivation of the p53 pathway in retinoblastoma. *Nature* 2006; **444**: 61–6.
22 Pereg Y, Shkedy D, de Graaf P *et al.* Phosphorylation of Hdmx mediates its Hdm2- and ATM-dependent degradation in response to DNA damage. *Proc Natl Acad Sci USA* 2005; **102**: 5056–61.

doi: 10.1111/j.1349-7006.2009.01180.x

23 Okamoto K, Kashima K, Pereg Y *et al.* DNA damage-induced phosphorylation of MdmX at serine 367 activates p53 by targeting MdmX for Mdm2-dependent degradation. *Mol Cell Biol* 2005; **25**: 9608–20.
24 Jin Y, Dai MS, Lu SZ *et al.* 14-3-3gamma binds to MDMX that is phosphorylated by UV-activated Chk1, resulting in p53 activation. *EMBO J* 2006; **25**: 1207–18.
25 Pereg Y, Lam S, Teunisse A *et al.* Differential roles of ATM- and Chk2-mediated phosphorylations of Hdmx in response to DNA damage. *Mol Cell Biol* 2006; **26**: 6819–31.
26 Chen L, Gilkes DM, Pan Y, Lane WS, Chen J. ATM and Chk2-dependent phosphorylation of MDMX contribute to p53 activation after DNA damage. *EMBO J* 2005; **24**: 3411–22.
27 Shmueli A, Oren M. Regulation of p53 by Mdm2: fate is in the numbers. *Mol Cell* 2004; **13**: 4–5.
28 Lopez-Pajares V, Kim MM, Yuan ZM. Phosphorylation of MDMX mediated by Akt leads to stabilization and induces 14-3-3 binding. *J Biol Chem* 2008; **283**: 13707–13.
29 Gu J, Nie L, Wiederschain D, Yuan ZM. Identification of p53 sequence elements that are required for MDM2-mediated nuclear export. *Mol Cell Biol* 2001; **21**: 8533–46.
30 Lohrum MA, Woods DB, Ludwig RL, Balint E, Vousden KH. C-terminal ubiquitination of p53 contributes to nuclear export. *Mol Cell Biol* 2001; **21**: 8521–32.
31 Xirodimas DP, Saville MK, Bourdon JC, Hay RT, Lane DP. Mdm2-mediated NEDD8 conjugation of p53 inhibits its transcriptional activity. *Cell* 2004; **118**: 83–97.
32 Toledo F, Wahl GM. Regulating the p53 pathway: *in vitro* hypotheses, *in vivo* veritas. *Nat Rev Cancer* 2006; **6**: 909–23.
33 Singh RK, Iyappan S, Scheffner M. Hetero-oligomerization with MdmX rescues the ubiquitin/Nedd8 ligase activity of RING finger mutants of Mdm2. *J Biol Chem* 2007; **282**: 10 901–7.
34 Becker K, Marchenko ND, Maurice M, Moll UM. Hyperubiquitylation of wild-type p53 contributes to cytoplasmic sequestration in neuroblastoma. *Cell Death Differ* 2007; **14**: 1350–60.
35 Moll UM, LaQuaglia M, Benard J, Riou G. Wild-type p53 protein undergoes cytoplasmic sequestration in undifferentiated neuroblastomas but not in differentiated tumors. *Proc Natl Acad Sci USA* 1995; **92**: 4407–11.
36 Lu W, Pochampally R, Chen L, Traidej M, Wang Y, Chen J. Nuclear exclusion of p53 in a subset of tumors requires MDM2 function. *Oncogene* 2000; **19**: 232–40.
37 Rodriguez-Lopez AM, Xenaki D, Eden TO, Hickman JA, Chresta CM. MDM2 mediated nuclear exclusion of p53 attenuates etoposide-induced apoptosis in neuroblastoma cells. *Mol Pharmacol* 2001; **59**: 135–43.
38 Danovi D, Meulmeester E, Pasini D *et al.* Amplification of Mdmx (or Mdm4) directly contributes to tumor formation by inhibiting p53 tumor suppressor activity. *Mol Cell Biol* 2004; **24**: 5835–43.
39 Jimenez GS, Khan SH, Stommel JM, Wahl GM. p53 regulation by post-translational modification and nuclear retention in response to diverse stresses. *Oncogene* 1999; **18**: 7656–65.
40 Li M, Brooks CL, Wu-Baer F, Chen D, Baer R, Gu W. Mono-versus polyubiquitination: differential control of p53 fate by Mdm2. *Science* 2003; **302**: 1972–5.
41 Li M, Brooks CL, Kon N, Gu W. A dynamic role of HAUSP in the p53–Mdm2 pathway. *Mol Cell* 2004; **13**: 879–86.
42 Meulmeester E, Maurice MM, Boutell C *et al.* Loss of HAUSP-mediated deubiquitination contributes to DNA damage-induced destabilization of Hdmx and Hdm2. *Mol Cell* 2005; **18**: 565–76.

Supporting Information

Additional Supporting Information may be found in the online version of this article:

Supporting Information Materials and Methods

Fig. S1. Non-phosphorylatable Mdmx cooperates with Mdm2 to suppress p53.

Fig. S2. Non-phosphorylatable Mdmx cooperates with Mdm2 to induce cytoplasmic localization of p53 in H1299.

Fig. S3. The Mdmx-3A mutation stimulates the localization of Mdm2 and p53 predominantly to the cytoplasm.

Fig. S4. Mdmx is required for cytoplasmic retention of p53 in neuroblastoma cells.

Please note: Wiley-Blackwell are not responsible for the content or functionality of any supporting materials supplied by the authors. Any queries (other than missing material) should be directed to the corresponding author for the article.

FEBS Letters 583 (2009) 2710–2714

FEBS Letters

journal homepage: www.FEBSLetters.org

Mdmx enhances p53 ubiquitination by altering the substrate preference of the Mdm2 ubiquitin ligase

Koji Okamoto [a,b,c], Yoichi Taya [b,c,1], Hitoshi Nakagama [a,*]

[a] National Cancer Center Research Institute, Early Oncogenesis Research Project, 5-1-1 Tsukiji, Chuo-ku, Tokyo 104-0045, Japan
[b] National Cancer Center Research Institute, Radiobiology Division, 5-1-1 Tsukiji, Chuo-ku, Tokyo 104-0045, Japan
[c] SORST, Japan Science and Technology Corporation, Japan

ARTICLE INFO

Article history:
Received 11 May 2009
Revised 26 June 2009
Accepted 13 July 2009
Available online 18 July 2009

Edited by Noboru Mizushima

Keywords:
Mdmx
Mdm2
p53
Ubiquitination

ABSTRACT

***mdm2* and *mdmx* oncogenes play essential yet non-redundant roles in synergistic inactivation of the tumor suppressor, p53. While Mdm2 inhibits p53 activity mainly by augmenting its ubiquitination, the functional role of Mdmx on p53 ubiquitination remains obscure. In transfected H1299 cells, Mdmx augmented Mdm2-mediated ubiquitination of p53. In in vitro ubiquitination assays, the Mdmx/Mdm2 heteromeric complex, in comparison to the Mdm2 homomer, showed enhanced ubiquitinase activity toward p53 and the reduced auto-ubiquitination of Mdm2. Alteration of the substrate specificity via binding to Mdmx may contribute to efficient ubiquitination and inactivation of p53 by Mdm2.**

Structured summary:
MINT-7219995: *P53* (uniprotkb:P04637) *physically interacts* (MI:0914) with *Ubiquitin* (uniprotkb:P62988) by *anti bait coimmunoprecipitation* (MI:0006)
MINT-7220023: *Ubiquitin* (uniprotkb:P62988) *physically interacts* (MI:0914) with *P53* (uniprotkb:P04637) by *pull down* (MI:0096)

1. Introduction

The p53 tumor suppressor protein plays a central role in preventing tumorigenesis. p53 functions as a sequence-specific transcriptional factor [1,2], and activated p53 exerts its function as a tumor suppressor by inducing numerous target genes [3–6]. In most cancer cells, its activity is lost via alteration of its gene or via other cellular events that inactivate p53 [7–9].

Mdm2 and Mdmx function as two major players in the suppression of p53 activity [10]. Accumulating reports indicate that the major function of Mdm2 in suppressing p53 is attributed to Mdm2-dependent p53 ubiquitination, which triggers proteasomal degradation or nuclear export of p53 [11], although it has been reported that Mdm2 inactivates p53 by other mechanisms [12–15]. Mdm2 possesses a RING finger domain, a protein–protein interaction motif that is found in many eukaryotic proteins and often possesses E3 ubiquitin ligase activity [16]. Indeed, Mdm2 functions as an E3 ubiquitin ligase, and the RING domain of Mdm2 is essential for its ubiquitin ligase activity toward p53 and Mdm2 itself [17–19].

Mdmx shares an extensive structural homology with Mdm2, and forms a heterodimer complex with Mdm2 through their RING finger domains [20,21], yet Mdmx in itself lacks the robust activity of an E3 ubiquitin ligase [22]. Thus, both genetic and biochemical evidence indicates that Mdmx and Mdm2 perform distinct yet co-operative functions in p53 inactivation.

Recent reports suggest that Mdmx may inactivate p53 by augmenting Mdm2-mediated ubiquitination of p53 [23–25]. However, precise mechanism by which Mdmx stimulates p53 ubiquitination by Mdm2 is not yet known.

In this paper, we demonstrated that wild-type Mdmx is capable of enhancing Mdm2-mediated p53 ubiquitination in vivo. Further, the in vitro study using purified Mdm2 or the Mdm2/Mdmx complex revealed that, when complexed with Mdmx, the extent of p53 ubiquitination by Mdm2 was enhanced while poly-ubiquitination of Mdm2 was significantly decreased. We propose that the effect of Mdmx on the preference of the substrate of the Mdm2 ubiquitin ligase plays an important role in effective ubiquitination of p53.

* Corresponding author.
E-mail address: hnakagam@ncc.go.jp (H. Nakagama).
[1] Present address: Cancer Science Institute of Singapore, National University of Singapore, Singapore 117456, Singapore.

0014-5793/$36.00 © 2009 Federation of European Biochemical Societies. Published by Elsevier B.V. All rights reserved.
doi:10.1016/j.febslet.2009.07.021

2. Materials and methods

2.1. DNA transfection

In DNA transfection experiments using H1299 cells, 2 μg of DNA and 4 μl of Lipofectamine 2000 reagent (Invitrogen) were introduced per 2.0×10^5 cells according to manufacturer's protocol. Cells were then incubated for 20 h before harvesting.

2.2. In vivo ubiquitination assay

For detection of p53 conjugated with endogenous ubiquitin, in vivo ubiquitination assays were performed as previously described [26] with some modifications. Transfected H1299 cells were lysed in SDS lysis buffer (50 mM Tris, pH 7.5, 100 mM NaCl, 1% SDS) supplemented with 1 mM DTT and protease inhibitor cocktail (PI) [27], boiled for 10 min, and diluted with ×4 volumes of dilution buffer (50 mM Tris, pH 7.5, 100 mM NaCl, 1.25% Triton X-100) supplemented with DTT and PI. After sonication of the lysates, p53 was immunoprecipitated with anti-p53 antibody (DO-1). Subsequently the immunoprecipitates were washed three times with 200-NP buffer [27], and analyzed by Western blotting with DO-1 and anti-ubiquitin antibody (FK2, MBL).

For detection of p53 conjugated with transfected $(His)_6$-ubiquitin, transfected H1299 cells were lysed in urea lysis buffer (100 mM NaH_2PO_4, 10 mM Tris–HCl, pH 8.0, 500 mM NaCl, 10% glycerol, 0.1% Triton X-100, 10 mM imidazole) supplemented with 10 mM β-mercaptoethanol, PI, 5 mM Iodoacetamide, and 1 mg/ml NEM. Proteins conjugated with His-tagged ubiquitin were purified as described before [28], and analyzed by Western blot analysis.

2.3. Protein expression and purification

Flag-tagged Human Mdm2 (Flag-Mdm2) or Human Mdmx RNA was transcribed from the corresponding cDNA using the Wheat Germ Expression Kit (Cell Free Science, Japan). Subsequently, the Flag-Mdm2 RNA alone or in combination with an excess amount of the Mdmx RNA was used for in vitro translation with wheat germ lysate (Cell Free Science) according to the manufacturer's instructions. Flag-Mdm2 or the Flag-Mdm2/Mdmx complex was then purified on agarose conjugated with anti-Flag antibody.

2.4. In vitro ubiquitination assay

In vitro ubiquitination assays were performed as previously described with some modifications [29]. Approximately 100 ng of Flag-Mdm2 or the Flag-Mdm2/Mdmx complex were mixed with the following purified components; 8 ng of GST-p53, 10 ng of E1 (Boston Biochem), 80 ng of E2 (UbcH5b, Boston Biochem), 3 μg of His-ubiquitin (Calbiochem), or methylated ubiquitin (Boston Biochem). In experiments shown in Fig. 4D, ^{125}I-ubiquitin (Perkin–Elmer) was included in the reaction mixture. These components were incubated in a reaction buffer (40 mM Tris–HCl, pH 7.5, 5 mM $MgCl_2$, 10 mM NaCl) in the presence of 2 mM Mg–ATP at 37 °C for the indicated times. After the reactions were terminated by adding SDS sample buffer, ubiquitinated proteins were separated in SDS–PAGE gels and detected by Western blot analyses or autoradiography.

3. Results

3.1. Wild-type Mdmx was capable of enhancing p53 ubiquitination in the presence of Mdm2 in vivo

Recently, we demonstrated that the non-phosphorylatable, active form of Mdmx augments p53 ubiquitination mediated by wild-type Mdm2 in transfected H1299 cells [30]. In order to determine whether wild-type Mdmx cooperates with Mdm2 to induce ubiquitination of p53 as well, wild-type Mdmx (Mdmx-wt) or the non-phosphorylated form of Mdmx (Mdmx-3A) was transfected together with Mdm2 into H1299 cells, and conjugation of p53 with endogenous ubiquitin was examined by Western blot analyses (Fig. 1). As expected from previous observation [30], Mdmx-3A, which is resistant to Mdm2-mediated ubiquitination and degradation, was expressed at higher levels than wild-type Mdmx (Fig. 1, lanes 2 and 3). p53 ubiquitination induced by Mdm2 was enhanced in the presence of co-transfected wild-type Mdmx (Fig. 1, lanes 5 and 8), indicating that wild-type Mdmx is capable of stimulating Mdm2-mediated ubiquitination of p53,

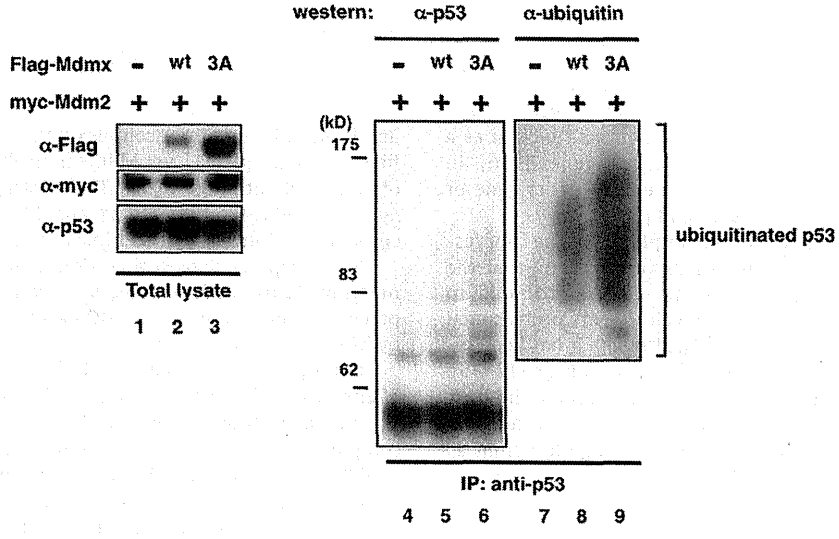

Fig. 1. Mdmx cooperates with Mdm2 to induce p53 ubiquitination. HA-p53 (0.15 mg) and either 0.4 mg of the control vector, wild-type Flag-Mdmx, or the Flag-Mdmx-3A mutant were transfected into H1299 cells in the presence of 0.2 mg of Myc-Mdm2. The total amount of transfected DNA was adjusted to 2 μg with pBluescript plasmid (Stratagene). Twenty hours after transfection, lysates prepared under denaturing conditions were used for immunoprecipitaiton with anti-p53 (DO-1) antibody. The immunoprecipitates were then used for Western blot analyses with DO-1 (left panel, and right bottom panel for low exposure) and with anti-ubiquitin antibody (right panel). Amounts of immunoprecipitates used for Western were normalized such that an equal amount of non-ubiquitinated p53 was loaded in each lane.

although the extent of the stimulation is less than that induced by the non-phosphorylatable mutant (Fig. 1, lanes 6 and 9).

3.2. Mutation at the C-terminal ubiquitinated lysines largely abolished p53 ubiquitination by Mdmx

It has been documented that Mdm2 ubiquitinates p53 at the six C-terminal lysines, the integrity of which are required for its nuclear export [31,32]. We created a mutant p53 in which all six lysines at the C-terminal domain (Fig. S1) were substituted by arginine (p53-K6R), and introduced wild-type p53 or the K6R mutant into H1299 cells together with Mdm2 in the presence or absence of Mdmx-3A. Examination of p53 ubiquitination in vivo revealed that the K6R mutation eliminates a majority of p53 ubiquitination enhanced by Mdmx (Fig. S2), indicating the six lysines were major sites for Mdmx-dependent ubiquitination.

3.3. Association of Mdmx with Mdm2 augments the ability of Mdm2 to ubiquitinate p53 and inhibits poly-ubiquitination of Mdm2 in vitro

In order to determine whether Mdmx enhances Mdm2-dependent ubiquitination of p53 via direct association with Mdm2, we next performed in vitro ubiquitination assays using purified recombinant proteins of Mdm2 or an Mdm2/Mdmx complex (see Section 2). Silver staining of the purified proteins indicated that the co-purified Mdmx formed a complex with Mdm2 at approximately a 1:1 molar ratio (Fig. 2A, right panel).

In order to determine the effect of the association with Mdmx on the activity of E3 ubiquitin ligase of Mdm2, homomeric Mdm2 or the Mdmx/Mdm2 complex was incubated with E1, E2 (UbcH5b), GST-p53, and ubiquitin, and time-course analyses of the ubiquitination of p53 and auto-ubiquitination of Mdm2 were simultaneously performed. The complex formation of Mdm2 with Mdmx-3A or with wild-type Mdmx resulted in an increase of p53 ubiquitination (Fig. 2B and C). In contrast, the Mdmx/Mdm2 complex showed a marked decrease in poly-ubiquitinated forms of Mdm2 in comparison to homomeric Mdm2 (Fig. 2B and C), indicating that the association with Mdmx-3A augments Mdm2-dependent p53 ubiquitination while it inhibits poly-ubiquitination of Mdm2.

3.4. Mdmx inhibits ubiquitination of the Mdm2-containing enzymatic complex

In order to confirm that Mdmx inhibits auto-ubiquitination of Mdm2, in vitro ubiquitination assays of the Mdm2 homomer or the Mdm2/Mdmx complex were performed in the presence of

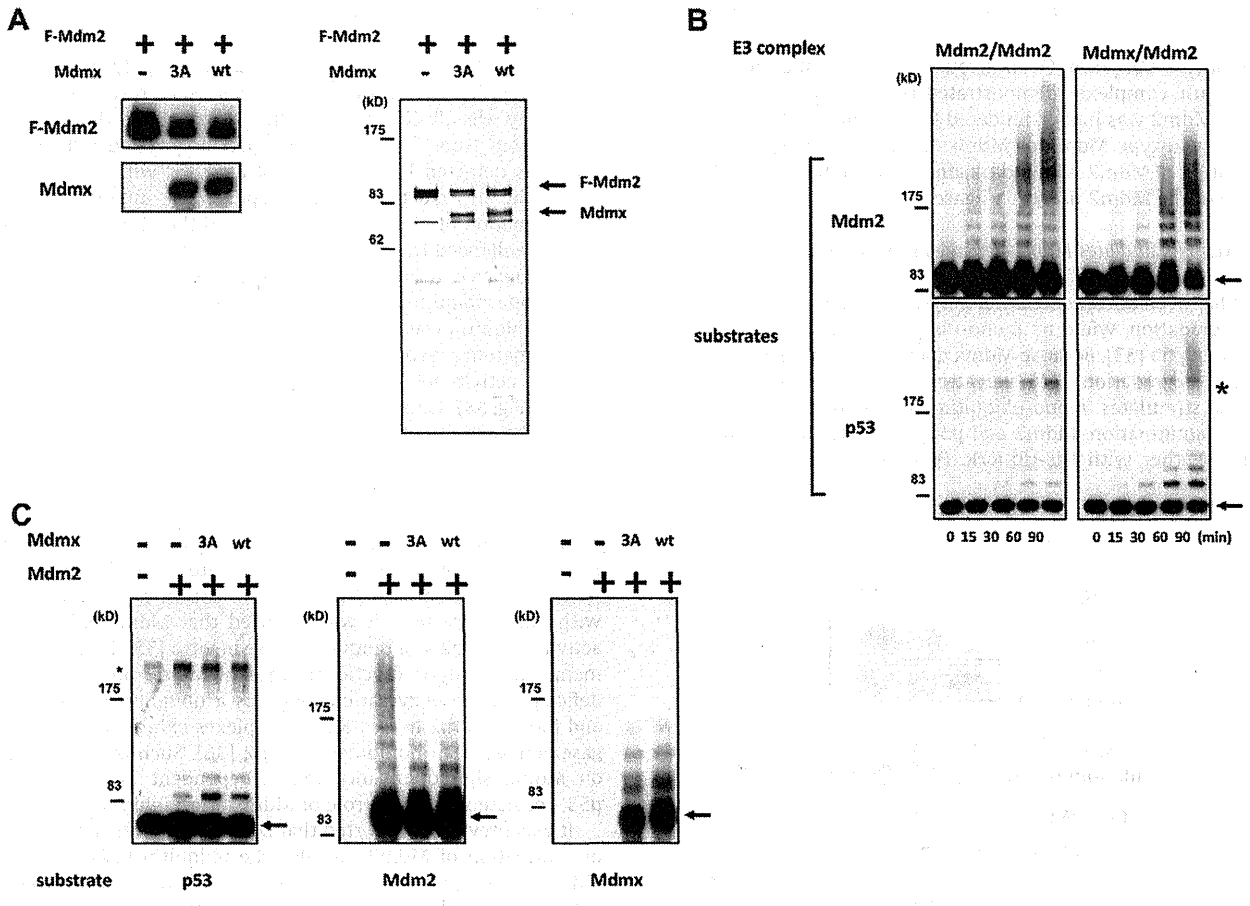

Fig. 2. Association of Mdmx with Mdm2 augments the activity of Mdm2 to ubiquitinate p53 and inhibits auto-ubiquitination of Mdm2 in vitro. (A) Purification of Mdm2 and the Mdm2/Mdmx complex. Flag-tagged Mdm2 was translated alone, or co-translated with Mdmx-3A or wild-type Mdmx in wheat germ lysates, as described in Section 2. The purified proteins were separated by10% SDS–PAGE, and detected by silver staining (right panel), or by Western blotting analyses with anti-Flag antibody (M2) or anti-Mdmx antibody (D-19) (left panel). (B) *In vitro* ubiquitination assays were performed with purified Mdm2 or Mdmx-3A/Mdm2. Ubiquitination reactions were terminated at the indicated times, and the extent of p53 ubiquitination and Mdm2 auto-ubiquitination was evaluated by Western blot analyses with anti-Flag antibody or anti-p53 antibody. The position of non-ubiquitinated substrates is designated by arrows. (C) In vitro ubiquitination assays were performed as described in (B), and the ubiquitination reactions were terminated after 30 min. Ubiquitination of Mdmx, p53, and Mdm2 was evaluated by Western blot analyses.

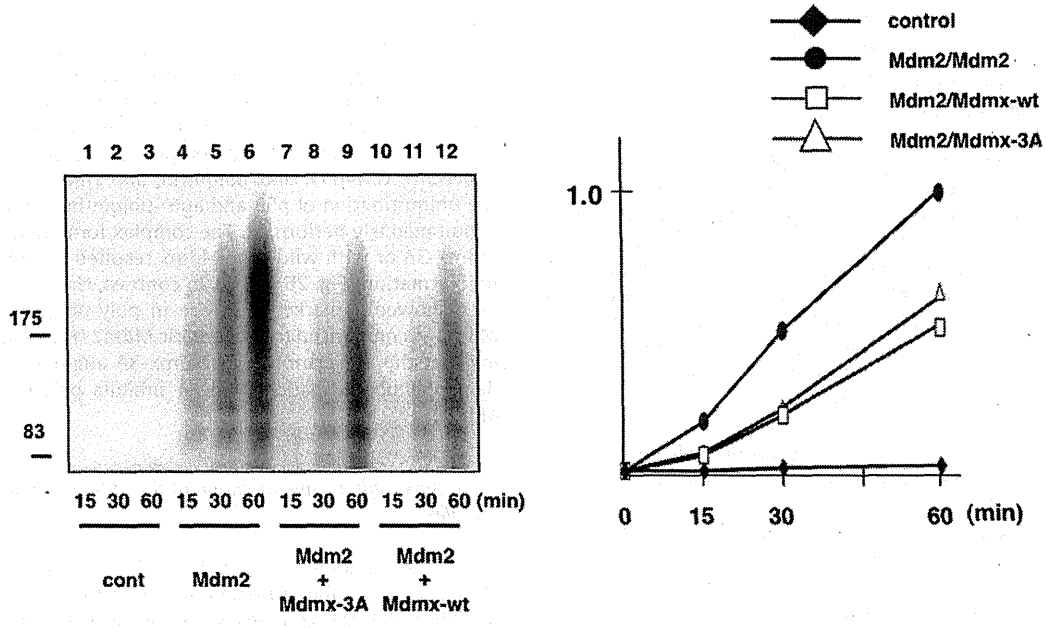

Fig. 3. In vitro ubiquitination reaction was performed as described in Fig. 2C, except that ^{125}I-labeled ubiquitin was included in the reaction. (left panel) Ubiquitinated Mdm2 or Mdm2/Mdmx was separated by 10% SDS–PAGE, and detected by autoradiography. Note that the ladder represents a mixture of ubiqutination of Mdm2 and Mdmx in lanes 7–12 (left panel). Levels of the ubiquitination were quantified and relative levels of ubiquitination were plotted (right panel).

^{125}I-labeled ubiquitin. Quantification of ubiquitin attached to the enzymatic complexes demonstrated that the auto-ubiquitination of the Mdm2 was indeed hindered by the complex formation with either wild-type Mdmx or Mdmx-3A (Fig. 3). Thus, the complex formation of Mdm2 with Mdmx affects the preference for the substrate of the Mdm2 ubiquitin ligase.

3.5. Mdmx stimulates Mdm2-dependent mono-ubiquitination of p53

It has been documented that poly-ubiquitination of p53 induces its degradation, while its mono-ubiquitnation stimulates nuclear export of p53 [33]. Because Mdmx does not significantly contribute to p53 degradation [34], we attempted to determine whether Mdmx stimulates mono-ubiquitination of p53 rather than its poly-ubiquitination. Mdm2 and p53 were introduced into H1299 cells together with His-Ub-K7R, $(His)_6$-tagged mutant ubiquitin which is not capable of forming a ladder of poly-ubiquitination due to arginine substitution in all seven lysine residues [29]. Subsequently, His-Ub-K7R was purified from lysates that were prepared from transfected cells, and p53 conjugated with His-Ub-7KR was detected by Western blot analyses with anti-p53 antibody. The introduction of wild-type Mdmx augmented mono-ubiquitination of p53 (Fig. 4, lane 2), and the Mdmx-3A mutation further enhanced the p53 mono-ubiquitination (Fig. 4, lane 3).

In order to determine whether Mdmx stimulates Mdm2-dependent mono-ubiquitination of p53 in vitro as well as in vivo, methylated ubiquitin was used instead of wild-type ubiquitin in in vitro ubiquitination assays. Indeed, the Mdmx/Mdm2 complex showed a stronger activity for p53 mono-ubiquitination than the homomeric Mdm2 (Fig. S3). Thus, the formation of a complex with Mdmx augments the activity of Mdm2 to mono-ubiquitinate p53.

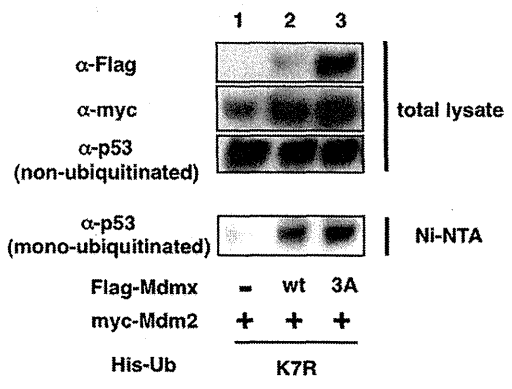

Fig. 4. Mdmx-3A or the control vector was transfected into H1299 cells together with Myc-Mdm2, HA-p53 and the indicated $(His)_6$-tagged ubiquitin K7R mutant. Twenty hours after transfection, cells were lysed with a buffer containing 6 M urea, and normalized lysates that contain equal amounts of non-ubiquitinated p53 were used to purify His-tagged ubiquitin on Ni-NTA agarose (QIAGEN). Ubiquitinated p53 was detected by Western blot analysis with anti-p53 antibody (DO-1).

4. Discussion

In this report, we demonstrated that wild-type Mdmx as well as its non-phosphorylatable mutant cooperates with Mdm2 to stimulate ubiquitination of p53 both in vivo and in vitro. In agreement with our observation, it was reported that Mdmx enhances the activity of Mdm2 as a ubiquitin ligase in vitro [35]. Mdmx complements the catalytic function of mutant Mdm2 proteins that are deficient in the enzymatic activity as a ubiquitin ligase [23–25] and Mdmx/Mdm2 hetero-RING complexes exhibit a greater E3 ligase activity than homomeric Mdm2 [36]. Such effects of Mdmx on Mdm2 should enhance Mdm2-dependent ubiquitination of p53, consistent with the role of Mdmx as an inhibitor of p53.

It was previously reported that Mdmx augments not only auto-ubiquitination of Mdm2 but also the ubiquitin ligase activity of Mdm2 toward p53 [35] in in vitro assays. However, auto-ubiquitination of the Mdm2 ubiquitin ligase negatively affects its activity because poly-ubiquitinated Mdm2 is targeted for proteasome-mediated degradation. Therefore, enhanced ubiquitinase activity of Mdm2 by Mdmx may not be translated into efficient stimulation of p53 ubiquitination if the association of Mdmx to Mdm2 simultaneously leads to stimulation of self-destruction of Mdm2. Our

observation that Mdmx inhibits poly-ubiquitination of Mdm2 while it stimulates p53 ubiquitination may attribute to a mechanism by which Mdmx stimulates Mdm2-dependent p53 ubiquitination without enhanced destruction of Mdm2, thus providing the molecular basis of how Mdmx cooperates with Mdm2 to inhibit p53 activity.

Recently Linke et al. reported the crystal structure of the heterodimer of Mdmx/Mdm2 RING domain, and proposed a model that favors transfer of ubiquitin to Mdmx that does not interact with E2 [37]. This can explain why Mdm2 is not extensively ubiquitinated in the Mdmx/Mdm2 heteromeric complex, thus providing mechanistic basis for reduced ubiquitination of Mdm2 in the Mdmx/Mdm2 complex (Fig. 2). It is noteworthy that, in in vitro ubiquitination assays, the levels of Mdm2 ubiquitination in the homomeric Mdm2 are higher than combined levels of ubiquitination of Mdm2 and Mdmx in the heteromeric complex (Fig. 3). Therefore, it is likely that Mdmx is relatively resistant to ubiquitination by bound Mdm2, unless Mdmx undergoes specific modification such as phosphorylation [27].

It is not clear at this moment how Mdmx stimulates Mdm2-mediated ubiquitination of p53. Mdm2 bound to Mdmx may position its catalytic domain more closer to the C-terminal domain of p53 than homomeric Mdm2, resulting in enhanced p53 ubiquitination. Alternatively, Mdm2 or Mdmx may compete with p53 as a substrate for Mdm2, and relative resistance of Mdmx against ubiquitination by bound Mdm2 may translate into facilitated p53 ubiquitination. Presumably, these two possibilities are not mutually exclusive, and combined effects of Mdmx on Mdm2-mediated ubiquitination may serve to stimulate ubiquitination and inactivation of p53.

Acknowledgements

We thank Aart Jochemsen for helpful suggestions. The His-ubiquitin expression plasmids were kind gifts from Wei Gu. We thank Kenji Kashima and Chihiro Ohtsubo for experimental assistance. This work was supported by a Grant-in-Aid for Scientific Research from the Ministry of Education, Culture, Sports, Science and Technology of Japan (Y.T and K.O.), a Grant-in-Aid for Third Term Comprehensive Control Research for Cancer from the Ministry of Health, Labor and Welfare, Japan (Y.T.), and the Foundation for Promotion of Cancer Research (K.O.).

Appendix A. Supplementary data

Supplementary data associated with this article can be found, in the online version, at doi:10.1016/j.febslet.2009.07.021.

References

[1] Levine, A.J. (1997) P53, the cellular gatekeeper for growth and division. Cell 88, 323–331.
[2] Laptenko, O. and Prives, C. (2006) Transcriptional regulation by p53: one protein, many possibilities. Cell Death Differ. 13, 951–961.
[3] Levine, A.J., Hu, W. and Feng, Z. (2006) The P53 pathway: what questions remain to be explored? Cell Death Differ. 13, 1027–1036.
[4] Oren, M. (2003) Decision making by p53: life, death and cancer. Cell Death Differ. 10, 431–442.
[5] Ko, L.J. and Prives, C. (1996) P53: puzzle and paradigm. Genes Dev. 10, 1054–1072.
[6] Vogelstein, B., Lane, D. and Levine, A.J. (2000) Surfing the p53 network. Nature 408, 307–310.
[7] Lozano, G. and Zambetti, G.P. (2005) What have animal models taught us about the p53 pathway? J. Pathol. 205, 206–220.
[8] Vousden, K.H. and Lu, X. (2002) Live or let die: the cell's response to p53. Nat. Rev. Cancer 2, 594–604.
[9] Olivier, M., Eeles, R., Hollstein, M., Khan, M.A., Harris, C.C. and Hainaut, P. (2002) The IARC TP53 database: new online mutation analysis and recommendations to users. Hum. Mutat. 19, 607–614.
[10] Marine, J.C., Francoz, S., Maetens, M., Wahl, G., Toledo, F. and Lozano, G. (2006) Keeping p53 in check: essential and synergistic functions of Mdm2 and Mdm4. Cell Death Differ. 13, 927–934.
[11] Michael, D. and Oren, M. (2003) The p53-Mdm2 module and the ubiquitin system. Semin. Cancer Biol. 13, 49–58.
[12] Momand, J., Zambetti, G.P., Olson, D.C., George, D. and Levine, A.J. (1992) The mdm-2 oncogene product forms a complex with the p53 protein and inhibits p53-mediated transactivation. Cell 69, 1237–1245.
[13] Oliner, J.D., Pietenpol, J.A., Thiagalingam, S., Gyuris, J., Kinzler, K.W. and Vogelstein, B. (1993) Oncoprotein MDM2 conceals the activation domain of tumour suppressor p53. Nature 362, 857–860.
[14] Ito, A., Lai, C.H., Zhao, X., Saito, S., Hamilton, M.H., Appella, E. and Yao, T.P. (2001) P300/CBP-mediated p53 acetylation is commonly induced by p53-activating agents and inhibited by MDM2. Embo J. 20, 1331–1340.
[15] Kobet, E., Zeng, X., Zhu, Y., Keller, D. and Lu, H. (2000) MDM2 inhibits p300-mediated p53 acetylation and activation by forming a ternary complex with the two proteins. Proc. Natl. Acad. Sci. USA 97, 12547–12552.
[16] Joazeiro, C.A. and Weissman, A.M. (2000) RING finger proteins: mediators of ubiquitin ligase activity. Cell 102, 549–552.
[17] Fang, S., Jensen, J.P., Ludwig, R.L., Vousden, K.H. and Weissman, A.M. (2000) Mdm2 is a RING finger-dependent ubiquitin protein ligase for itself and p53. J. Biol. Chem. 275, 8945–8951.
[18] Honda, R. and Yasuda, H. (2000) Activity of MDM2, a ubiquitin ligase, toward p53 or itself is dependent on the RING finger domain of the ligase. Oncogene 19, 1473–1476.
[19] Honda, R., Tanaka, H. and Yasuda, H. (1997) Oncoprotein MDM2 is a ubiquitin ligase E3 for tumor suppressor p53. FEBS Lett. 420, 25–27.
[20] Tanimura, S., Ohtsuka, S., Mitsui, K., Shirouzu, K., Yoshimura, A. and Ohtsubo, M. (1999) MDM2 interacts with MDMX through their RING finger domains. FEBS Lett. 447, 5–9.
[21] Sharp, D.A., Kratowicz, S.A., Sank, M.J. and George, D.L. (1999) Stabilization of the MDM2 oncoprotein by interaction with the structurally related MDMX protein. J. Biol. Chem. 274, 38189–38196.
[22] Stad, R., Little, N.A., Xirodimas, D.P., Frenk, R., van der Eb, A.J., Lane, D.P., Saville, M.K. and Jochemsen, A.G. (2001) Mdmx stabilizes p53 and Mdm2 via two distinct mechanisms. EMBO Rep. 2, 1029–1034.
[23] Singh, R.K., Iyappan, S. and Scheffner, M. (2007) Hetero-oligomerization with MdmX rescues the ubiquitin/Nedd8 ligase activity of RING finger mutants of Mdm2. J. Biol. Chem. 282, 10901–10907.
[24] Uldrijan, S., Pannekoek, W.J. and Vousden, K.H. (2007) An essential function of the extreme C-terminus of MDM2 can be provided by MDMX. Embo J. 26, 102–112.
[25] Poyurovsky, M.V., Priest, C., Kentsis, A., Borden, K.L., Pan, Z.Q., Pavletich, N. and Prives, C. (2007) The Mdm2 RING domain C-terminus is required for supramolecular assembly and ubiquitin ligase activity. Embo J. 26, 90–101.
[26] Carter, S., Bischof, O., Dejean, A. and Vousden, K.H. (2007) C-terminal modifications regulate MDM2 dissociation and nuclear export of p53. Nat. Cell Biol. 9, 428–435.
[27] Okamoto, K., Kashima, K., Pereg, Y., Ishida, M., Yamazaki, S., Nota, A., Teunisse, A., Migliorini, D., Kitabayashi, I., Marine, J.C., Prives, C., Shiloh, Y., Jochemsen, A.G. and Taya, Y. (2005) DNA damage-induced phosphorylation of MdmX at serine 367 activates p53 by targeting MdmX for Mdm2-dependent degradation. Mol. Cell Biol. 25, 9608–9620.
[28] de Graaf, P., Little, N.A., Ramos, Y.F., Meulmeester, E., Letteboer, S.J. and Jochemsen, A.G. (2003) Hdmx protein stability is regulated by the ubiquitin ligase activity of Mdm2. J. Biol. Chem. 278, 38315–38324.
[29] Li, M., Brooks, C.L., Wu-Baer, F., Chen, D., Baer, R. and Gu, W. (2003) Mono- versus polyubiquitination: differential control of p53 fate by Mdm2. Science 302, 1972–1975.
[30] Ohtsubo, C., Shiokawa, D., Kodama, M., Gaiddon, C., Nakagama, H., Jochemsen, A.G., Taya, Y. and Okamoto, K. (2009) Cytoplasmic tethering is involved in synergistic inhibition of p53 by Mdmx and Mdm2. Cancer Sci.
[31] Gu, J., Nie, L., Wiederschain, D. and Yuan, Z.M. (2001) Identification of p53 sequence elements that are required for MDM2-mediated nuclear export. Mol. Cell Biol. 21, 8533–8546.
[32] Lohrum, M.A., Woods, D.B., Ludwig, R.L., Balint, E. and Vousden, K.H. (2001) C-terminal ubiquitination of p53 contributes to nuclear export. Mol. Cell Biol. 21, 8521–8532.
[33] Shmueli, A. and Oren, M. (2004) Regulation of p53 by Mdm2: fate is in the numbers. Mol. Cell 13, 4–5.
[34] Toledo, F., Krummel, K.A., Lee, C.J., Liu, C.W., Rodewald, L.W., Tang, M. and Wahl, G.M. (2006) A mouse p53 mutant lacking the proline-rich domain rescues Mdm4 deficiency and provides insight into the Mdm2-Mdm4-p53 regulatory network. Cancer Cell 9, 273–285.
[35] Linares, L.K., Hengstermann, A., Ciechanover, A., Muller, S. and Scheffner, M. (2003) HdmX stimulates Hdm2-mediated ubiquitination and degradation of p53. Proc. Natl. Acad. Sci. USA 100, 12009–12014.
[36] Kawai, H., Lopez-Pajares, V., Kim, M.M., Wiederschain, D. and Yuan, Z.M. (2007) RING domain-mediated interaction is a requirement for MDM2's E3 ligase activity. Cancer Res. 67, 6026–6030.
[37] Linke, K., Mace, P.D., Smith, C.A., Vaux, D.L., Silke, J. and Day, C.L. (2008) Structure of the MDM2/MDMX RING domain heterodimer reveals dimerization is required for their ubiquitylation in trans. Cell Death Differ.

LETTERS

Frequent inactivation of A20 in B-cell lymphomas

Motohiro Kato[1,2], Masashi Sanada[1,5], Itaru Kato[6], Yasuharu Sato[7], Junko Takita[1,2,3], Kengo Takeuchi[8], Akira Niwa[6], Yuyan Chen[1,2], Kumi Nakazaki[1,4,5], Junko Nomoto[9], Yoshitaka Asakura[9], Satsuki Muto[1], Azusa Tamura[1], Mitsuru Iio[1], Yoshiki Akatsuka[11], Yasuhide Hayashi[12], Hiraku Mori[13], Takashi Igarashi[2], Mineo Kurokawa[4], Shigeru Chiba[3], Shigeo Mori[14], Yuichi Ishikawa[8], Koji Okamoto[10], Kensei Tobinai[9], Hitoshi Nakagama[10], Tatsutoshi Nakahata[6], Tadashi Yoshino[7], Yukio Kobayashi[9] & Seishi Ogawa[1,5]

A20 is a negative regulator of the NF-κB pathway and was initially identified as being rapidly induced after tumour-necrosis factor-α stimulation[1]. It has a pivotal role in regulation of the immune response and prevents excessive activation of NF-κB in response to a variety of external stimuli[2–7]; recent genetic studies have disclosed putative associations of polymorphic *A20* (also called *TNFAIP3*) alleles with autoimmune disease risk[8,9]. However, the involvement of A20 in the development of human cancers is unknown. Here we show, using a genome-wide analysis of genetic lesions in 238 B-cell lymphomas, that *A20* is a common genetic target in B-lineage lymphomas. A20 is frequently inactivated by somatic mutations and/or deletions in mucosa-associated tissue lymphoma (18 out of 87; 21.8%) and Hodgkin's lymphoma of nodular sclerosis histology (5 out of 15; 33.3%), and, to a lesser extent, in other B-lineage lymphomas. When re-expressed in a lymphoma-derived cell line with no functional *A20* alleles, wild-type A20, but not mutant A20, resulted in suppression of cell growth and induction of apoptosis, accompanied by downregulation of NF-κB activation. The A20-deficient cells stably generated tumours in immunodeficient mice, whereas the tumorigenicity was effectively suppressed by re-expression of A20. In A20-deficient cells, suppression of both cell growth and NF-κB activity due to re-expression of A20 depended, at least partly, on cell-surface-receptor signalling, including the tumour-necrosis factor receptor. Considering the physiological function of A20 in the negative modulation of NF-κB activation induced by multiple upstream stimuli, our findings indicate that uncontrolled signalling of NF-κB caused by loss of A20 function is involved in the pathogenesis of subsets of B-lineage lymphomas.

Malignant lymphomas of B-cell lineages are mature lymphoid neoplasms that arise from various lymphoid tissues[10,11]. To obtain a comprehensive registry of genetic lesions in B-lineage lymphomas, we performed a single nucleotide polymorphism (SNP) array analysis of 238 primary B-cell lymphoma specimens of different histologies, including 64 samples of diffuse large B-cell lymphomas (DLBCLs), 52 follicular lymphomas, 35 mantle cell lymphomas (MCLs), and 87 mucosa-associated tissue (MALT) lymphomas (Supplementary Table 1). Three Hodgkin's-lymphoma-derived cell lines were also analysed. Interrogating more than 250,000 SNP sites, this platform permitted the identification of copy number changes at an average resolution of less than 12 kilobases (kb). The use of large numbers of SNP-specific probes is a unique feature of this platform, and combined with the CNAG/AsCNAR software, enabled accurate determination of 'allele-specific' copy numbers, and thus allowed for sensitive detection of loss of heterozygosity (LOH) even without apparent copy-number reduction, in the presence of up to 70–80% normal cell contamination[12,13].

Lymphoma genomes underwent a wide range of genetic changes, including numerical chromosomal abnormalities and segmental gains and losses of chromosomal material (Supplementary Fig. 1), as well as copy-number-neutral LOH, or uniparental disomy (Supplementary Fig. 2). Each histology type had a unique genomic signature, indicating a distinctive underlying molecular pathogenesis for different histology types (Fig. 1a and Supplementary Fig. 3). On the basis of the genomic signatures, the initial pathological diagnosis of MCL was re-evaluated and corrected to DLBCL in two cases. Although most copy number changes involved large chromosomal segments, a number of regions showed focal gains and deletions, accelerating identification of their candidate gene targets. After excluding known copy number variations, we identified 46 loci showing focal gains (19 loci) or deletions (27 loci) (Supplementary Tables 2 and 3 and Supplementary Fig. 4).

Genetic lesions on the NF-κB pathway were common in B-cell lymphomas and found in approximately 40% of the cases (Supplementary Table 1), underpinning the importance of aberrant NF-κB activation in lymphomagenesis[11,14] in a genome-wide fashion. They included focal gain/amplification at the *REL* locus (16.4%) (Fig. 1b) and *TRAF6* locus (5.9%), as well as focal deletions at the *PTEN* locus (5.5%) (Supplementary Figs 1 and 4). However, the most striking finding was the common deletion at 6q23.3 involving a 143-kb segment. It exclusively contained the *A20* gene (also called *TNFAIP3*), a negative regulator of NF-κB activation[3–7,15] (Fig. 1b), which was previously reported as a candidate target of 6q23 deletions in ocular lymphoma[16]. LOH involving the *A20* locus was found in 50 cases, of which 12 showed homozygous deletions as determined by the loss of both alleles in an allele-specific copy number analysis (Fig. 1b, Table 1 and Supplementary Table 4). On the basis of this finding, we searched for possible tumour-specific mutations of *A20* by genomic DNA sequencing of entire coding exons of the gene in the same series of lymphoma samples (Supplementary Fig. 5). Because two out of the three Hodgkin's-lymphoma-derived cell lines had biallelic *A20* deletions/mutations (Supplementary Fig. 6), 24 primary samples from Hodgkin's lymphoma were also analysed for mutations, where

[1]Cancer Genomics Project, Department of [2]Pediatrics, [3]Cell Therapy and Transplantation Medicine, and [4]Hematology and Oncology, Graduate School of Medicine, University of Tokyo, 7-3-1 Hongo, Bunkyo-ku, Tokyo 113-8655, Japan. [5]Core Research for Evolutional Science and Technology, Japan Science and Technology Agency, 4-1-8, Honcho, Kawaguchi-shi, Saitama 332-0012, Japan. [6]Department of Pediatrics, Graduate School of Medicine, Kyoto University, 54 Kawahara-cho, Shogoin, Sakyo-ku, Kyoto 606-8507, Japan. [7]Department of Pathology, Okayama University Graduate School of Medicine, Dentistry and Pharmaceutical Sciences, 2-5-1 Shikata-cho, Kita-ku, Okayama 700-8558, Japan. [8]Division of Pathology, The Cancer Institute of Japanese Foundation for Cancer Research, Japan, 3-10-6 Ariake, Koto-ku, Tokyo 135-8550, Japan. [9]Hematology Division, Hospital, and [10]Early Oncogenesis Research Project, Research Institute, National Cancer Center, 5-1-1 Tsukiji, Chuo-ku, Tokyo 104-0045, Japan. [11]Division of Immunology, Aichi Cancer Center Research Institute, 1-1 Kanokoden, Chikusa-ku, Nagoya 464-8681, Japan. [12]Gunma Children's Medical Center, 779 Shimohakoda, Hokkitsu-machi, Shibukawa 377-8577, Japan. [13]Division of Hematology, Internal Medicine, Showa University Fujigaoka Hospital, 1-30, Fujigaoka, Aoba-ku, Yokohama-shi, Kanagawa 227-8501, Japan. [14]Department of Pathology, Teikyo University School of Medicine, 2-11-1 Kaga, Itabashi-ku, Tokyo 173-8605, Japan.

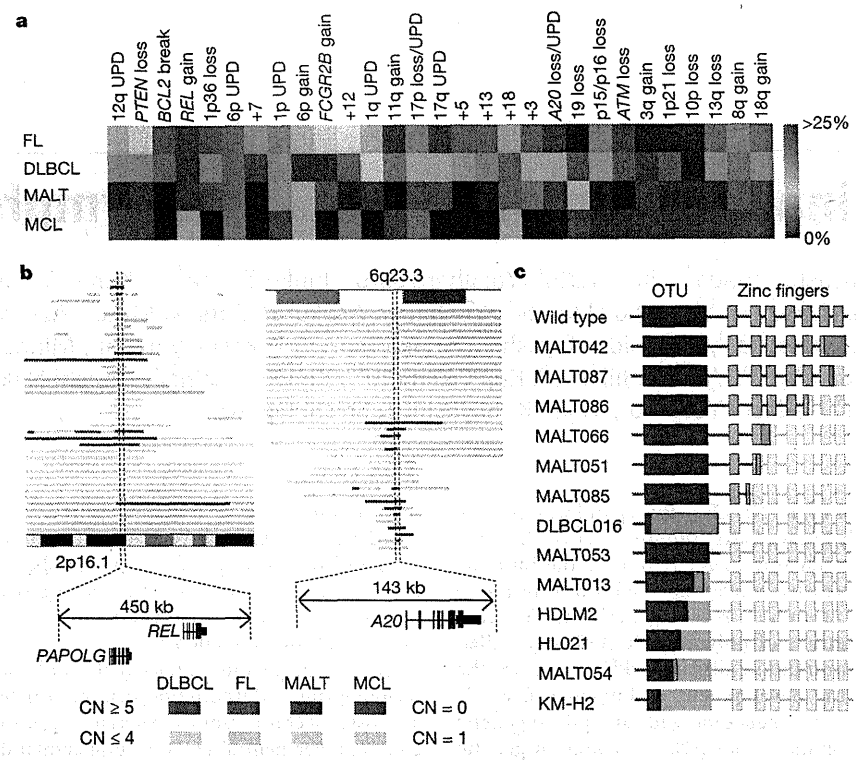

Figure 1 | Genomic signatures of different B-cell lymphomas and common genetic lesions at 2p16-15 and 6q23.3 involving NF-κB pathway genes. **a**, Twenty-nine genetic lesions were found in more than 10% in at least one histology and used for clustering four distinct histology types of B-lineage lymphomas. The frequency of each genetic lesion in each histology type is colour-coded. FL, follicular lymphoma; UPD, uniparental disomy. **b**, Recurrent genetic changes are depicted based on CNAG output of the SNP array analysis of 238 B-lineage lymphoma samples, which include gains at the *REL* locus on 2p16-15 (left panel) and the *A20* locus on 6q23.3 (right panel). Regions showing copy number gain or loss are indicated by horizontal lines. Four histology types are indicated by different colours, where high-grade amplifications and homozygous deletions are shown by darker shades to discriminate from simple gains (copy number ≤4) and losses (copy number = 1) (lighter shades). **c**, Point mutations and small nucleotide insertions and deletions in the *A20* (*TNFAIP3*) gene caused premature truncation of A20 in most cases. Altered amino acids caused by frame shifts are indicated by green bars.

genomic DNA was extracted from 150 microdissected CD30-positive tumour cells (Reed–Sternberg cells) for each sample. *A20* mutations were found in 18 out of 265 lymphoma samples (6.8%) (Table 1), among which 13 mutations, including nonsense mutations (3 cases), frame-shift insertions/deletions (9 cases), and a splicing donor site mutation (1 case) were thought to result in premature termination of translation (Fig. 1c). Four missense mutations and one intronic mutation were identified in five microdissected Hodgkin's lymphoma samples. They were not found in the surrounding normal tissues, and thus, were considered as tumour-specific somatic changes.

In total, biallelic *A20* lesions were found in 31 out of 265 lymphoma samples including 3 Hodgkin's lymphoma cell lines. Quantitative analysis of SNP array data suggested that these *A20* lesions were present in the major tumour fraction within the samples (Supplementary Fig. 7). Inactivation of *A20* was most frequent in MALT lymphoma (18 out of 87) and Hodgkin's lymphoma (7 out of 27), although it was also found in DLBCL (5 out of 64) and follicular lymphoma (1 out of 52) at lower frequencies. In MALT lymphoma, biallelic *A20* lesions were confirmed in 18 out of 24 cases (75.0%) with LOH involving the 6q23.3 segment (Supplementary Fig. 8). Considering the limitation in detecting very small homozygous deletions, *A20* was thought to be the target of 6q23 LOH in MALT lymphoma. On the other hand, the 6q23 LOHs in other histology types tended to be extended into more centromeric regions and less frequently accompanied biallelic *A20* lesions (Supplementary Fig. 8 and Supplementary Table 4), indicating that they might be more heterogeneous with regard to their gene targets. We were unable to analyse Hodgkin's lymphoma samples using SNP arrays owing to insufficient genomic DNA obtained from microdissected samples, and were likely to underestimate the frequency of *A20* inactivation in Hodgkin's lymphoma because we might fail to detect a substantial proportion of cases with homozygous deletions, which explained 50% (12 out of 24) of *A20* inactivation in other histology types. *A20* mutations in Hodgkin's lymphoma were exclusively found in nodular sclerosis classical Hodgkin's lymphoma (5 out of 15) but not in other histology types (0 out of 9), although the possible association requires further confirmation in additional cases.

A20 is a key regulator of NF-κB signalling, negatively modulating NF-κB activation through a wide variety of cell surface receptors and viral proteins, including tumour-necrosis factor (TNF) receptors, toll-like receptors, CD40, as well as Epstein–Barr-virus-associated LMP1 protein[2,5,17,18]. To investigate the role of A20 inactivation in lymphomagenesis, we re-expressed wild-type A20 under a *Tet*-inducible promoter in a lymphoma-derived cell line (KM-H2) that had no functional *A20* alleles (Supplementary Fig. 6), and examined the effect of A20 re-expression on cell proliferation, survival and downstream NF-κB signalling pathways. As shown in Fig. 2a–c and Supplementary Fig. 9, re-expression of wild-type A20 resulted in the suppression of cell proliferation and enhanced apoptosis, and in the concomitant accumulation of IκBβ and IκBε, and downregulation of NF-κB activity. In contrast, re-expression of two lymphoma-derived A20 mutants, $A20^{532Stop}$ or $A20^{750Stop}$, failed to show growth suppression, induction of apoptosis, accumulation of IκBβ and IκBε or downregulation of

Table 1 | Inactivation of A20 in B-lineage lymphomas

Histology	Tissue	Sample	Allele	Uniparental disomy	Exon	Mutation	Biallelic inactivation
DLBCL							5 out of 64 (7.8%)
	Lymph node	DLBCL008	−/−	No	–	–	
	Lymph node	DLBCL016	+/−	No	Ex2	329insA	
	Lymph node	DLBCL022	−/−	No	–	–	
	Lymph node	DLBCL028	−/−	Yes	–	–	
	Lymph node	MCL008*	−/−	Yes	–	–	
Follicular lymphoma							1 out of 52 (1.9%)
	Lymph node	FL024	−/−	No	–	–	
MCL							0 out of 35 (0%)
MALT							18 out of 87 (21.8%)
Stomach							3 out of 23 (13.0%)
	Gastric mucosa	MALT013	+/+	Yes	Ex5	705insG	
	Gastric mucosa	MALT014	+/+	Yes	Ex3	Ex3 donor site>A	
	Gastric mucosa	MALT036	+/−	No	Ex7	delintron6-Ex7†	
Eye							13 out of 43 (30.2%)
	Ocular adnexa	MALT008	−/−	No	–	–	
	Ocular adnexa	MALT017	−/−	No	–	–	
	Ocular adnexa	MALT051	+/−	No	Ex7	1943delTG	
	Ocular adnexa	MALT053	+/+	Yes	Ex6	1016G>A(stop)	
	Ocular adnexa	MALT054	+/−	No	Ex3	502delTC	
	Ocular adnexa	MALT055	−/−	No	–	–	
	Ocular adnexa	MALT066	+/−	No	Ex7	1581insA	
	Ocular adnexa	MALT067	−/−	No	–	–	
	Ocular adnexa	MALT082	−/−	Yes	–	–	
	Ocular adnexa	MALT084	−/−	Yes	–	–	
	Ocular adnexa	MALT085	+/+	Yes	Ex7	1435insG	
	Ocular adnexa	MALT086	+/+	Yes	Ex6	878C>T(stop)	
	Ocular adnexa	MALT087	+/+	Yes	Ex9	2304delGG	
Lung							2 out of 12 (16.7%)
	Lung	MALT042	−/−	No	–	–	
	Lung	MALT047	+/+	Yes	Ex9	2281insT	
Other‡							0 out of 9 (0%)
Hodgkin's lymphoma							7 out of 27 (26.0%)
NSHL	Lymph node	HL10	ND	ND	Ex7	1777G>A(V571I)	
NSHL	Lymph node	HL12	ND	ND	Ex7	1156A>G(R364G)	
NSHL	Lymph node	HL21	ND	ND	Ex4	569G>A(stop)	
NSHL	Lymph node	HL24	ND	ND	Ex3	1487C>A(T474N)	
NSHL	Lymph node	HL23	ND	ND	–	Intron 3§	
	Cell line	KM-H2	−/−	No	–		
	Cell line	HDLM2	+/−	No	Ex4	616ins29bp‖	
Total							31 out of 265 (11.7%)

DLBCL, diffuse large B-cell lymphoma; MALT, MALT lymphoma; MCL, mantle cell lymphoma; ND, not determined because SNP array analysis was not performed; NSHL, nodular sclerosis classical Hodgkin's lymphoma.
* Diagnosis was changed based on the genomic data, which was confirmed by re-examination of pathology.
† Deletion including the boundary of intron 6 and exon 7 (see also Supplementary Fig. 5b).
‡ Including 1 parotid gland, 1 salivary gland, 2 colon and 5 thyroid cases.
§ Insertion of CTC at −19 bases from the beginning of exon 3.
‖ Insertion of TGGCTTCCACAGACACACCCATGGCCCGA.

NF-κB activity (Fig. 2a–c), indicating that these were actually loss-of-function mutations. To investigate the role of A20 inactivation in lymphomagenesis *in vivo*, *A20*- and mock-transduced KM-H2 cells were transplanted in NOD/SCID/γ_c^{null} (NOG) mice[19], and their tumour formation status was examined for 5 weeks with or without induction of wild-type A20 by tetracycline administration. As shown in Fig. 2d, mock-transduced cells developed tumours at the injected sites, whereas the *Tet*-inducible *A20*-transduced cells generated tumours only in the absence of A20 induction (Supplementary Table 5), further supporting the tumour suppressor role of A20 in lymphoma development.

Given the mode of negative regulation of NF-κB signalling, we next investigated the origins of NF-κB activity that was deregulated by A20 loss in KM-H2 cells. The conditioned medium prepared from a 48-h serum-free KM-H2 culture had increased NF-κB upregulatory activity compared with fresh serum-free medium, which was inhibited by re-expression of A20 (Fig. 3a). KM-H2 cells secreted two known ligands for TNF receptor—TNF-α and lymphotoxin-α (Supplementary Fig. 10)[20]—and adding neutralizing antibodies against these cytokines into cultures significantly suppressed their cell growth and NF-κB activity without affecting the levels of their overall suppression after A20 induction (Fig. 3b, d). In addition, recombinant TNF-α and/or lymphotoxin-α added to fresh serum-free medium promoted cell growth and NF-κB activation in KM-H2 culture, which were again suppressed by re-expression of A20 (Fig. 3c, e). Although our data in Fig. 3 also show the presence of factors other than TNF-α and lymphotoxin-α in the KM-H2-conditioned medium—as well as some intrinsic pathways in the cell (Fig. 3a)—that were responsible for the A20-dependent NF-κB activation, these results indicate that both cell growth and NF-κB activity that were upregulated by A20 inactivation depend at least partly on the upstream stimuli that evoked the NF-κB-activating signals.

Aberrant activation of the NF-κB pathway is a hallmark of several subtypes of B-lineage lymphomas, including Hodgkin's lymphoma, MALT lymphoma, and a subset of DLBCL, as well as other lymphoid neoplasms[11,14], where a number of genetic alterations of NF-κB signalling pathway genes[21–25], as well as some viral proteins[26,27], have been implicated in the aberrant activation of the NF-κB pathway[14]. Thus, frequent inactivation of A20 in Hodgkin's lymphoma and MALT and other lymphomas provides a novel insight into the molecular pathogenesis of these subtypes of B-lineage lymphomas through deregulated NF-κB activation. Because A20 provides a

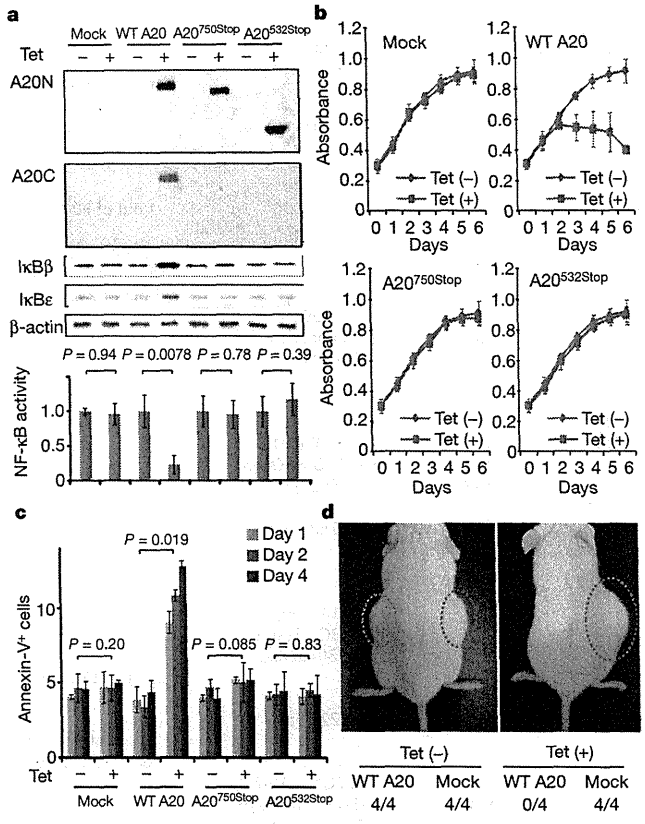

Figure 2 | Effects of wild-type and mutant A20 re-expressed in a lymphoma cell line that lacks the normal *A20* gene. a, Western blot analyses of wild-type (WT) and mutant ($A20^{532Stop}$ and $A20^{750Stop}$) A20, as well as IκBβ and IκBε, in KM-H2 cells, in the presence or absence of tetracycline treatment (top panels). A20N and A20C are polyclonal antisera raised against N-terminal and C-terminal A20 peptides, respectively. β-actin blots are provided as a control. NF-κB activities are expressed as mean absorbance ± s.d. ($n = 6$) in luciferase assays (bottom panel). **b,** Proliferation of KM-H2 cells stably transduced with plasmids for mock and *Tet*-inducible wild-type A20, $A20^{532Stop}$ and $A20^{750Stop}$ was measured using a cell counting kit in the presence (red lines) or absence (blue lines) of tetracycline. Mean absorbance ± s.d. ($n = 5$) is plotted. **c,** The fractions of Annexin-V-positive KM-H2 cells transduced with various *Tet*-inducible A20 constructs were measured by flow cytometry after tetracycline treatment and the mean values (±s.d., $n = 3$) are plotted. **d,** *In vivo* tumorigenicity was assayed by inoculating 7×10^6 KM-H2 cells transduced with mock or *Tet*-inducible wild-type A20 in NOG mice, with (right panel) or without (left panel) tetracycline administration.

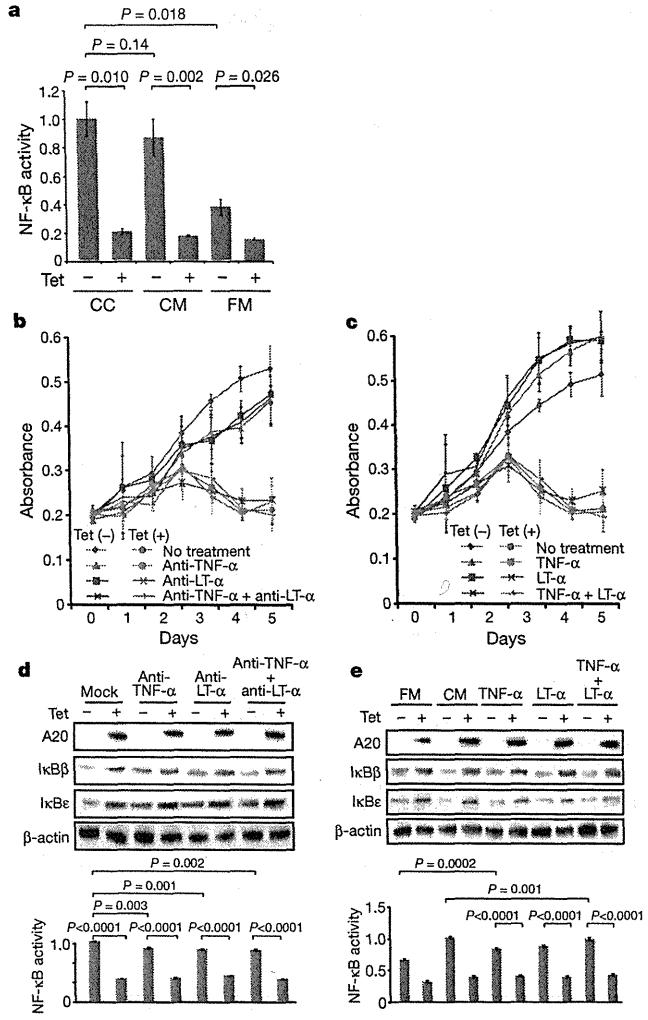

Figure 3 | Tumour suppressor role of A20 under external stimuli. a, NF-κB activity in KM-H2 cells was measured 30 min after cells were inoculated into fresh medium (FM) or KM-H2-conditioned medium (CM) obtained from the 48-h culture of KM-H2, and was compared with the activity after 48 h continuous culture of KM-H2 (CC). A20 was induced 12 h before inoculation in Tet (+) groups. **b, c,** Effects of neutralizing antibodies against TNF-α and lymphotoxin-α (LTα) (**b**) and of recombinant TNF-α and LT-α added to the culture (**c**) on cell growth were evaluated in the presence (Tet (+)) or absence (Tet (−)) of A20 induction. Cell numbers were measured using a cell counting kit and are plotted as their mean absorbance ± s.d. ($n = 6$). **d, e,** Effects of the neutralizing antibodies (**d**) and the recombinant cytokines added to the culture (**e**) on NF-κB activities and the levels of IκBβ and IκBε after 48 h culture with (Tet (+)) or without (Tet (−)) tetracycline treatment. NF-κB activities are expressed as mean absorbance ± s.d. ($n = 6$) in luciferase assays.

negative feedback mechanism in the regulation of NF-κB signalling pathways upon a variety of stimuli, aberrant activation of NF-κB will be a logical consequence of A20 inactivation. However, there is also the possibility that the aberrant NF-κB activity of A20-inactivated lymphoma cells is derived from upstream stimuli, which may be from the cellular environment. In this context, it is intriguing that MALT lymphoma usually arises at the site of chronic inflammation caused by infection or autoimmune disorders and may show spontaneous regression after eradication of infectious organisms[28]; furthermore, Hodgkin's lymphoma frequently shows deregulated cytokine production from Reed–Sternberg cells and/or surrounding reactive cells[29]. Detailed characterization of the NF-κB pathway regulated by A20 in both normal and neoplastic B lymphocytes will promote our understanding of the precise roles of A20 inactivation in the pathogenesis of these lymphoma types. Our finding underscores the importance of genome-wide approaches in the identification of genetic targets in human cancers.

METHODS SUMMARY

Genomic DNA from 238 patients with non-Hodgkin's lymphoma and three Hodgkin's-lymphoma-derived cell lines was analysed using GeneChip SNP genotyping microarrays (Affymetrix). This study was approved by the ethics boards of the University of Tokyo, National Cancer Institute Hospital, Okayama University, and the Cancer Institute of the Japanese Foundation of Cancer Research. After appropriate normalization of mean array intensities, signal ratios between tumours and anonymous normal references were calculated in an allele-specific manner, and allele-specific copy numbers were inferred from the observed signal ratios based on the hidden Markov model using CNAG/AsCNAR software (http://www.genome.umin.jp). *A20* mutations were examined by directly sequencing genomic DNA using a set of primers (Supplementary Table 6). Full-length cDNAs of wild-type and mutant *A20* were introduced into a

lentivirus vector, pLenti4/TO/V5-DEST (Invitrogen), with a *Tet*-inducible promoter. Viral stocks were prepared by transfecting the vector plasmids into 293FT cells (Invitrogen) using the calcium phosphate method and then infected to the KM-H2 cell line. Proliferation of KM-H2 cells was measured using a Cell Counting Kit (Dojindo). Western blot analyses and luciferase assays were performed as previously described. NF-κB activity was measured by luciferase assays in KM-H2 cells stably transduced with a reporter plasmid having an NF-κB response element, pGL4.32 (Promega). Apoptosis of KM-H2 upon A20 induction was evaluated by counting Annexin-V-positive cells by flow cytometry. For *in vivo* tumorigenicity assays, 7×10^6 KM-H2 cells were transduced with the *Tet*-inducible *A20* gene and those with a mock vector were inoculated on the contralateral sides in eight NOG mice[19] and examined for their tumour formation with ($n = 4$) or without ($n = 4$) tetracycline administration. Full copy number data of the 238 lymphoma samples will be accessible from the Gene Expression Omnibus (GEO, http://ncbi.nlm.nih.gov/geo/) with the accession number GSE12906.

Full Methods and any associated references are available in the online version of the paper at www.nature.com/nature.

Received 17 September 2008; accepted 3 March 2009.
Published online 3 May 2009.

1. Dixit, V. M. *et al.* Tumor necrosis factor-α induction of novel gene products in human endothelial cells including a macrophage-specific chemotaxin. *J. Biol. Chem.* **265,** 2973–2978 (1990).
2. Song, H. Y., Rothe, M. & Goeddel, D. V. The tumor necrosis factor-inducible zinc finger protein A20 interacts with TRAF1/TRAF2 and inhibits NF-κB activation. *Proc. Natl Acad. Sci. USA* **93,** 6721–6725 (1996).
3. Lee, E. G. *et al.* Failure to regulate TNF-induced NF-κB and cell death responses in A20-deficient mice. *Science* **289,** 2350–2354 (2000).
4. Boone, D. L. *et al.* The ubiquitin-modifying enzyme A20 is required for termination of Toll-like receptor responses. *Nature Immunol.* **5,** 1052–1060 (2004).
5. Wang, Y. Y., Li, L., Han, K. J., Zhai, Z. & Shu, H. B. A20 is a potent inhibitor of TLR3- and Sendai virus-induced activation of NF-κB and ISRE and IFN-β promoter. *FEBS Lett.* **576,** 86–90 (2004).
6. Wertz, I. E. *et al.* De-ubiquitination and ubiquitin ligase domains of A20 downregulate NF-κB signalling. *Nature* **430,** 694–699 (2004).
7. Heyninck, K. & Beyaert, R. A20 inhibits NF-κB activation by dual ubiquitin-editing functions. *Trends Biochem. Sci.* **30,** 1–4 (2005).
8. Graham, R. R. *et al.* Genetic variants near *TNFAIP3* on 6q23 are associated with systemic lupus erythematosus. *Nature Genet.* **40,** 1059–1061 (2008).
9. Musone, S. L. *et al.* Multiple polymorphisms in the *TNFAIP3* region are independently associated with systemic lupus erythematosus. *Nature Genet.* **40,** 1062–1064 (2008).
10. Jaffe, E. S., Harris, N. L., Stein, H. & Vardiman, J. W. *World Health Organization Classification of Tumours. Pathology and Genetics of Tumours of Hematopoietic and Lymphoid Tissues* (IARC Press, 2001).
11. Klein, U. & Dalla-Favera, R. Germinal centres: role in B-cell physiology and malignancy. *Nature Rev. Immunol.* **8,** 22–33 (2008).
12. Nannya, Y. *et al.* A robust algorithm for copy number detection using high-density oligonucleotide single nucleotide polymorphism genotyping arrays. *Cancer Res.* **65,** 6071–6079 (2005).
13. Yamamoto, G. *et al.* Highly sensitive method for genomewide detection of allelic composition in nonpaired, primary tumor specimens by use of affymetrix single-nucleotide-polymorphism genotyping microarrays. *Am. J. Hum. Genet.* **81,** 114–126 (2007).
14. Jost, P. J. & Ruland, J. Aberrant NF-κB signaling in lymphoma: mechanisms, consequences, and therapeutic implications. *Blood* **109,** 2700–2707 (2007).
15. Durkop, H., Hirsch, B., Hahn, C., Foss, H. D. & Stein, H. Differential expression and function of A20 and TRAF1 in Hodgkin lymphoma and anaplastic large cell lymphoma and their induction by CD30 stimulation. *J. Pathol.* **200,** 229–239 (2003).
16. Honma, K. *et al. TNFAIP3* is the target gene of chromosome band 6q23.3-q24.1 loss in ocular adnexal marginal zone B cell lymphoma. *Genes Chromosom. Cancer* **47,** 1–7 (2008).
17. Sarma, V. *et al.* Activation of the B-cell surface receptor CD40 induces A20, a novel zinc finger protein that inhibits apoptosis. *J. Biol. Chem.* **270,** 12343–12346 (1995).
18. Fries, K. L., Miller, W. E. & Raab-Traub, N. The A20 protein interacts with the Epstein-Barr virus latent membrane protein 1 (LMP1) and alters the LMP1/TRAF1/TRADD complex. *Virology* **264,** 159–166 (1999).
19. Hiramatsu, H. *et al.* Complete reconstitution of human lymphocytes from cord blood $CD34^+$ cells using the NOD/SCID/γ^{null} mice model. *Blood* **102,** 873–880 (2003).
20. Hsu, P. L. & Hsu, S. M. Production of tumor necrosis factor-α and lymphotoxin by cells of Hodgkin's neoplastic cell lines HDLM-1 and KM-H2. *Am. J. Pathol.* **135,** 735–745 (1989).
21. Dierlamm, J. *et al.* The apoptosis inhibitor gene *API2* and a novel 18q gene, *MLT*, are recurrently rearranged in the t(11;18)(q21;q21) associated with mucosa-associated lymphoid tissue lymphomas. *Blood* **93,** 3601–3609 (1999).
22. Willis, T. G. *et al.* Bcl10 is involved in t(1;14)(p22;q32) of MALT B cell lymphoma and mutated in multiple tumor types. *Cell* **96,** 35–45 (1999).
23. Joos, S. *et al.* Classical Hodgkin lymphoma is characterized by recurrent copy number gains of the short arm of chromosome 2. *Blood* **99,** 1381–1387 (2002).
24. Martin-Subero, J. I. *et al.* Recurrent involvement of the *REL* and *BCL11A* loci in classical Hodgkin lymphoma. *Blood* **99,** 1474–1477 (2002).
25. Lenz, G. *et al.* Oncogenic *CARD11* mutations in human diffuse large B cell lymphoma. *Science* **319,** 1676–1679 (2008).
26. Deacon, E. M. *et al.* Epstein-Barr virus and Hodgkin's disease: transcriptional analysis of virus latency in the malignant cells. *J. Exp. Med.* **177,** 339–349 (1993).
27. Yin, M. J. *et al.* HTLV-I Tax protein binds to MEKK1 to stimulate IκB kinase activity and NF-κB activation. *Cell* **93,** 875–884 (1998).
28. Isaacson, P. G. & Du, M. Q. MALT lymphoma: from morphology to molecules. *Nature Rev. Cancer* **4,** 644–653 (2004).
29. Skinnider, B. F. & Mak, T. W. The role of cytokines in classical Hodgkin lymphoma. *Blood* **99,** 4283–4297 (2002).

Supplementary Information is linked to the online version of the paper at www.nature.com/nature.

Acknowledgements This work was supported by the Core Research for Evolutional Science and Technology, Japan Science and Technology Agency, by the 21st century centre of excellence program 'Study on diseases caused by environment/genome interactions', and by Grant-in-Aids from the Ministry of Education, Culture, Sports, Science and Technology of Japan and from the Ministry of Health, Labor and Welfare of Japan for the 3rd-term Comprehensive 10-year Strategy for Cancer Control. We also thank Y. Ogino, E. Matsui and M. Matsumura for their technical assistance.

Author Contributions M.Ka., K.N. and M.S. performed microarray experiments and subsequent data analyses. M.Ka., Y.C., K.Ta., J.T., J.N., M.I., A.T. and Y.K. performed mutation analysis of *A20*. M.Ka., S.Mu., M.S., Y.C. and Y.Ak. conducted functional assays of mutant A20. Y.S., K.Ta., Y.As., H.M., M.Ku., S.Mo., S.C., Y.K., K.To. and Y.I. prepared tumour specimens. I.K., K.O., A.N., H.N. and T.N. conducted *in vivo* tumorigenicity experiments in NOG/SCID mice. T.I., Y.H., T.Y., Y.K. and S.O. designed overall studies, and S.O. wrote the manuscript. All authors discussed the results and commented on the manuscript.

Author Information The copy number data as well as the raw microarray data will be accessible from the GEO (http://ncbi.nlm.nih.gov/geo/) with the accession number GSE12906. Reprints and permissions information is available at www.nature.com/reprints. Correspondence and requests for materials should be addressed to S.O. (sogawa-tky@umin.ac.jp) or Y.K. (ykkobaya@ncc.go.jp).

METHODS

Specimens. Primary tumour specimens were obtained from patients who were diagnosed with DLBCL, follicular lymphoma, MCL, MALT lymphoma, or classical Hodgkin's lymphoma. In total, 238 primary lymphoma specimens listed in Supplementary Table 1 were subjected to SNP array analysis. Three Hodgkin's-lymphoma-derived cell lines (KM-H2, HDLM2, L540) were obtained from Hayashibara Biochemical Laboratories, Inc., Fujisaki Cell Center and were also analysed by SNP array analysis.

Microarray analysis. High-molecular-mass DNA was isolated from tumour specimens and subjected to SNP array analysis using GeneChip Mapping 50K and/or 250K arrays (Affymetrix). The scanned array images were processed with Gene Chip Operation software (GCOS), followed by SNP calls using GTYPE. Genome-wide copy number measurements and LOH detection were performed using CNAG/AsCNAR software[12,13].

Mutation analysis. Mutations in the *A20* gene were examined in 265 samples of B-lineage lymphoma, including 62 DLBCLs, 52 follicular lymphomas, 87 MALTs, 37 MCLs and 3 Hodgkin's-lymphoma-derived cell lines and 24 primary Hodgkin's lymphoma samples, by direct sequencing using an ABI PRISM 3130xl Genetic Analyser (Applied Biosystems). To analyse primary Hodgkin's lymphoma samples in which CD30-positive tumour cells (Reed–Sternberg cells) account for only a fraction of the specimen, 150 Reed–Sternberg cells were collected for each 10 μm slice of a formalin-fixed block immunostained for CD30 by laser-capture microdissection (ASLMD6000, Leica), followed by genomic DNA extraction using QIAamp DNA Micro kit (Qiagen). The primer sets used in this study are listed in Supplementary Table 6.

Functional analysis of wild-type and mutant A20. Full-length cDNA for wild-type *A20* was isolated from total RNA extracted from an acute myeloid leukaemia-derived cell line, CTS, and subcloned into a lentivirus vector (pLenti4/TO/V5-DEST, Invitrogen). cDNAs for mutant A20 were generated by PCR amplification using mutagenic primers (Supplementary Table 6), and introduced into the same lentivirus vector. Forty-eight hours after transfection of each plasmid into 293FT cells using the calcium phosphate method, lentivirus stocks were obtained from ultrafiltration using Amicon Ultra (Millipore), and used to infect KM-H2 cells to generate stable transfectants of mock, wild-type and mutant A20. Each KM-H2 derivative cell line was further transduced stably with a reporter plasmid (pGL4.32, Promega) containing a luciferase gene under an NF-κB-responsive element by electroporation using Nucleofector reagents (Amaxa).

Assays for cell proliferation and NF-κB activity. Proliferation of the KM-H2 derivative cell lines was assayed in triplicate using a Cell Counting Kit (Dojindo). The mean absorption of five independent assays was plotted with s.d. for each derivative line. Two independent KM-H2-derived cell lines were used for each experiment. The NF-κB activity in KM-H2 derivatives for A20 mutants was evaluated by luciferase assays using a PiccaGene Luciferase Assay Kit (TOYO B-Net Co.). Each assay was performed in triplicate and the mean absorption of five independent experiments was plotted with s.d.

Western blot analyses. Polyclonal anti-sera against N-terminal (anti-A20N) and C-terminal (anti-A20C) A20 peptides were generated by immunizing rabbits with these peptides (LSNMRKAVKIRERTPEDIC for anti-A20N and CFQFKQMYG for anti-A20C, respectively). Total cell lysates from KM-H2 cells were separated on 7.5% polyacrylamide gel and subjected to western blot analysis using antibodies to A20 (anti-A20N and anti-A20C), IκBα (sc-847), IκBβ (sc-945), IκBγ (sc-7155) and actin (sc-8432) (Santa Cruz Biotechnology).

Functional analyses of wild-type and mutant A20. Each KM-H2 derivative cell line stably transduced with various *Tet*-inducible A20 constructs was cultured in serum-free medium in the presence or absence of A20 induction using 1 μg ml^{-1} of tetracycline, and cell number was counted every day. 1×10^6 cells of each KM-H2 derivative cell line were analysed for their intracellular levels of IκBβ and IκBε and for NF-κB activities by western blot analyses and luciferase assays, respectively, 12 h after the beginning of cell culture. Effects of human recombinant TNF-α and lymphotoxin-α (210-TA and 211-TB, respectively, R&D Systems) on the NF-κB pathway and cell proliferation were evaluated by adding both cytokines into 10 ml of serum-free cell culture at a concentration of 200 pg ml^{-1}. For cell proliferation assays, culture medium was half replaced every 12 h to minimize the side-effects of autocrine cytokines. Intracellular levels of IκBβ, IκBε and NF-κB were examined 12 h after the beginning of the cell culture. To evaluate the effect of neutralizing TNF-α and lymphotoxin-α, 1×10^6 of KM-H2 cells transduced with both *Tet*-inducible A20 and the NF-κB-luciferase reporter were pre-cultured in serum-free media for 36 h, and thereafter neutralizing antibodies against TNF-α (MAB210, R&D Systems) and/or lymphotoxin-α (AF-211-NA, R&D Systems) were added to the media at a concentration of 200 pg ml^{-1}. After the extended culture during 12 h with or without 1 μg ml^{-1} tetracycline, the intracellular levels of IκBβ and IκBε and NF-κB activities were examined by western blot analysis and luciferase assays, respectively. To examine the effects of A20 re-expression on apoptosis, 1×10^6 KM-H2 cells were cultured for 4 days in 10 ml medium with or without *Tet* induction. After staining with phycoerythrin-conjugated anti-Annexin-V (ID556422, Becton Dickinson), Annexin-V-positive cells were counted by flow cytometry at the indicated times.

***In vivo* tumorigenicity assays.** KM-H2 cells transduced with a mock or *Tet*-inducible wild-type *A20* gene were inoculated into NOG mice and their tumorigenicity was examined for 5 weeks with or without tetracycline administration. Injections of 7×10^6 cells of each KM-H2 cell line were administered to two opposite sites in four mice. Tetracycline was administered in drinking water at a concentration of 200 μg ml^{-1}.

ELISA. Concentrations of TNF-α, lymphotoxin-α, IL-1, IL-2, IL-4, IL-6, IL-12, IL-18 and TGF-β in the culture medium were measured after 48 h using ELISA. For those cytokines detectable after 48-h culture (TNFα, LTα, and IL-6), their time course was examined further using the Quantikine ELISA kit (R&D Systems).

Statistical analysis. Significance of the difference in NF-κB activity between two given groups was evaluated using a paired *t*-test, in which the data from each independent luciferase assay were paired to calculate test statistics. To evaluate the effect of A20 re-expression in KM-H2 cells on apoptosis, the difference in the fractions of Annexin-V-positive cells between Tet (+) and Tet (−) groups was also tested by a paired *t*-test for assays, in which the data from the assays performed on the same day were paired.

GASTROENTEROLOGY 2009;136:1012–1024

EpCAM-Positive Hepatocellular Carcinoma Cells Are Tumor-Initiating Cells With Stem/Progenitor Cell Features

TARO YAMASHITA,* JUNFANG JI,* ANURADHA BUDHU,* MARSHONNA FORGUES,* WEN YANG,‡ HONG-YANG WANG,‡ HULIANG JIA,§ QINGHAI YE,§ LUN-XIU QIN,§ ELAINE WAUTHIER,‖ LOLA M. REID,‖ HIROSHI MINATO,¶ MASAO HONDA,¶ SHUICHI KANEKO,¶ ZHAO-YOU TANG,§ and XIN WEI WANG*

*Liver Carcinogenesis Section, Laboratory of Human Carcinogenesis, Center for Cancer Research, National Cancer Institute, Bethesda, Maryland; ‡International Cooperation Laboratory on Signal Transduction, Eastern Hepatobiliary Surgery Institute, Shanghai, China; §Liver Cancer Institute and Zhongshan Hospital, Fudan University, Shanghai, China; ‖Department of Cell and Molecular Physiology, University of North Carolina School of Medicine, Chapel Hill, North Carolina; and the ¶Liver Disease Center and Kanazawa University Hospital, Kanazawa University, Kanazawa, Japan

Background & Aims: **Cancer progression/metastases and embryonic development share many properties including cellular plasticity, dynamic cell motility, and integral interaction with the microenvironment. We hypothesized that the heterogeneous nature of hepatocellular carcinoma (HCC), in part, may be owing to the presence of hepatic cancer cells with stem/progenitor features.** ***Methods:*** **Gene expression profiling and immunohistochemistry analyses were used to analyze 235 tumor specimens derived from 2 recently identified HCC subtypes (EpCAM$^+$ α-fetoprotein [AFP$^+$] HCC and EpCAM$^-$ AFP$^-$ HCC). These subtypes differed in their expression of AFP, a molecule produced in the developing embryo, and EpCAM, a cell surface hepatic stem cell marker. Fluorescence-activated cell sorting was used to isolate EpCAM$^+$ HCC cells, which were tested for hepatic stem/progenitor cell properties.** ***Results:*** **Gene expression and pathway analyses revealed that the EpCAM$^+$ AFP$^+$ HCC subtype had features of hepatic stem/progenitor cells. Indeed, the fluorescence-activated cell sorting–isolated EpCAM$^+$ HCC cells displayed hepatic cancer stem cell–like traits including the abilities to self-renew and differentiate. Moreover, these cells were capable of initiating highly invasive HCC in nonobese diabetic, severe combined immunodeficient mice. Activation of Wnt/β-catenin signaling enriched the EpCAM$^+$ cell population, whereas RNA interference-based blockage of EpCAM, a Wnt/β-catenin signaling target, attenuated the activities of these cells.** ***Conclusions:*** **Taken together, our results suggest that HCC growth and invasiveness is dictated by a subset of EpCAM$^+$ cells, opening a new avenue for HCC cancer cell eradication by targeting Wnt/β-catenin signaling components such as EpCAM.**

Tumors originate from normal cells as a result of accumulated genetic/epigenetic changes. Although considered monoclonal in origin, tumor cells are heterogeneous in their morphology, clinical behavior, and molecular profiles.[1,2] Tumor cell heterogeneity has been explained previously by the clonal evolution model[3]; however, recent evidence has suggested that heterogeneity may be owing to derivation from endogenous stem/progenitor cells[4] or de-differentiation of a transformed cell.[5] This hypothesis supports an early proposal that cancers represent "blocked ontogeny"[6] and a derivative that cancers are transformed stem cells.[7] This renaissance of stem cells as targets of malignant transformation has led to realizations about the similarities between cancer cells and normal stem cells in their capacity to self-renew, produce heterogeneous progenies, and limitlessly divide.[8] The cancer stem cell (CSC) (or tumor-initiating cell) concept is that a subset of cancer cells bear stem cell features that are indispensable for a tumor. Accumulating evidence suggests the involvement of CSCs in the perpetuation of various cancers including leukemia, breast cancer, brain cancer, prostate cancer, and colon cancer.[9–13] Experimentally, putative CSCs have been isolated using cell surface markers specific for normal stem cells. Stem cell–like features of CSC have been confirmed by functional in vitro clonogenicity and in vivo tumorigenicity assays. For example, leukemia-initiating cells in nonobese diabetic, severe combined immunodeficient (NOD/SCID) mice are CD34^{++}CD38$^-$.[11] Breast cancer CSCs are CD44$^+$CD24$^{-/low}$ cells, whereas tumor-initiating cells of the brain, colon, and prostate are CD133$^+$.[10,12,13] CSCs are considered more metastatic and drug-/radiation-resistant than non-CSCs in the tumor, and are responsible for cancer relapse. These findings warrant the development of treatment strategies that can specifically eradicate CSCs.[14,15]

Abbreviations used in this paper: AFP, α-fetoprotein; BIO, 6-bromoindirubin-3′-oxime; CSC, cancer stem cell; FACS, fluorescence-activated cell sorting; 5-FU, 5-fluorouracil; HpSC, hepatic stem cell; IF, immunofluorescence; IHC, immunohistochemistry; MACS, magnetic-activated cell sorting; MeBIO, 1-methyl-BIO; MH, mature hepatocyte; PCNA, proliferating cell nuclear antigen; siRNA, small interfering RNA.

0016-5085/09/$36.00
doi:10.1053/j.gastro.2008.12.004